JAERI-Tech
94-018

THE PLASMA POSITION CONTROL OF ITER EDA PLASMA

September 1994

Ikuo SENDA[*1], Satoshi NISHIO, Toshihide TSUNEMATSU
Toru NISHINO[*2] and Hirobumi FUJIEDA[*3]

日本原子力研究所
Japan Atomic Energy Research Institute

本レポートは，日本原子力研究所が不定期に公刊している研究報告書です。

入手の問合わせは，日本原子力研究所技術情報部情報資料課（〒319-11 茨城県那珂郡東海村）あて，お申し越しください。なお，このほかに財団法人原子力弘済会資料センター（〒319-11 茨城県那珂郡東海村日本原子力研究所内）で複写による実費頒布をおこなっております。

This report is issued irregularly.

Inquiries about availability of the reports should be addressed to Information Division, Department of Technical Information, Japan Atomic Energy Research Institute, Tokai-mura, Naka-gun, Ibaraki-ken 319-11, Japan.

編集兼発行　日本原子力研究所

印　　刷　㈱原子力資料サービス

The Plasma Position Control of ITER EDA Plasma

Ikuo SENDA*1, Satoshi NISHIO, Toshihide TSUNEMATSU
Toru NISHINO*2 and Hirobumi FUJIEDA*3

Department of ITER Project
Naka Fusion Research Establishment
Japan Atomic Energy Research Institute
Naka-machi, Naka-gun, Ibaraki-ken

(Received August 19, 1994)

The study on the plasma position control of ITER EDA performed by Japan Home Team during the sensitivity study in 1994 is summarized. The controllabilities of plasmas in the Outline Design and elongated version are compared. The model used to describe the motion of the plasma is a rigid model. The PD feedback control is applied with respect to the displacements of the plasma from the equilibrium. Three types of fluctuations, which initiate the motion of the plasma, are examined, namely a finite horizontal fluctuation field, a small horizontal fluctuation field such that the motion of the plasma is governed by the passive structures and an abrupt change of the poloidal beta β_p and internal inductance ℓ_i. In the simulations of finite horizontal fluctuation fields, controls depend on the strength of the fluctuations, for instance, 3-5V is needed for 5-10G of fluctuation fields in the Outline Design. When the fluctuation field is small and the plasma displacement grows in a characteristic time of the passive structures, a few volt of the control voltage is enough to obtain good controllability. It is shown that the control when (β_p, ℓ_i) changes simultaneously is demanding and a large control voltage is required to maintain satisfactory control. Comparing the elongated version with the Outline Design, the control voltage which is larger than the Outline Design by a factor of 2-3 is required to obtain the same controllability in the elongated version.

Keywords: ITER, EDA, Position Control, Control Voltage, PD Control

---

*1 On loan from Toshiba Corporation
*2 Kanazawa Computer Service
*3 Atomic Energy General Services Corporation

ITER－EDAプラズマの位置制御

日本原子力研究所那珂研究所ITER開発室
仙田　郁夫[*1]・西尾　敏・常松　俊秀
西野　徹[*2]・藤枝　浩文[*3]

（1994年8月19日受理）

ITER EDA感度解析に於いて，日本国内設計チームが行ったプラズマ位置制御シミュレーションをまとめる。標準設計と高非円形度設計のプラズマ位置制御性を比較・検討した。解析に用いたモデルは，プラズマの形状を固定した剛体プラズマモデルである。プラズマ位置の平衡からのずれに対して，比例・微分制御利得を用いたフィードバック制御を行った。プラズマの位置が平衡からずれる原因として，有限の水平擾乱磁場，プラズマの運動に影響を与えないほど小さな水平擾乱磁場，及びプラズマポロイダルベータ値（β_p,）・内部インダクタンス（ℓ_i）の急激な変化の三種類を検討した。有限の水平擾乱磁場を加えたシミュレーションの場合，制御性はその擾乱磁場の強さに依存する。5－10ガウスの擾乱磁場を加えた場合，3－5Vの制御電圧が必要である。十分小さな水平擾乱磁場によりプラズマの運動が始まる場合，プラズマの揺らぎは真空容器等の構造物に誘起される渦電流で決まる時定数で成長し，数ボルトの制御電圧で十分な制御性が得られる。一方，（β_p, ℓ_i）同時かつ短時間の内に変化した場合，大きな制御電圧を要する。標準設計と高非円形度設計を比較した場合，高非円形度プラズマの制御では，同等の制御性を得るために標準設計の2－3倍の制御電圧が必要となる。

那珂研究所：〒311－01　茨城県那珂郡那珂町大字向山801－1
＊1　㈱東芝より出向中
＊2　㈱カナザワコンピュータサービス
＊3　㈱原子力資料サービス

目　　次

Contents

1. Introduction

According to the request of the International Thermonuclear Experimental Reactor (ITER) Council, the sensitivity study was undertaken by the Joint Central Team in collaboration with four parties' Home Teams. The objectives of the sensitivity study was to determine the relative importance of different design parameters in determining the over all ITER construction cost. During the works, it was noticed that the vertical stabilities of plasma was one of the critical issues for determining the construction cost. As a part of the sensitivity study, therefore the analysis on the plasma position control and the assessment of the required power supply were carried out. This paper is the summary of the plasma position control analysis performed by Japan Home Team.

The plasma position control is related to various aspects of the fusion reactor design[1-3]. First of all, it is important to maintain the discharge in a suitable condition, which is required by the scenario of the discharge. The position control provides an important requirement to determine the facility of the power supply system. The demand on the position control also has a determining impact on the structures surrounding the plasma, such as the blanket and vacuum vessel. The characteristic time of the plasma without passive structures is the Alfven time, which is an order of micro second. However due to the eddy current induced in the passive structures, the characteristic time of the motion of the plasma is reduced to that determined by the passive structures and the active control of the plasma becomes possible. Thus, the concept of the plasma control provides a restriction on the design of the blanket and the vacuum vessel and the materials to build them. Another important issue is the Control loss(AC loss). Due to the magnetic field of the plasma control, the eddy currents are induced in the conductors and the other structures. Since the superconducting magnets are considered in the ITER design, this AC loss has a serious impact on the cryogenic system of ITER. In this way, the plasma position control has intimate relations to the designs and costs of the other components.

ITER has two goals to be achieved. One of them is to

demonstrate the controlled ignition of the duration for more than 1000 seconds. The other is the extended burn of the plasma with steady state as an ultimate goal. In the sensitivity study, the possibility of reducing the major plasma parameters was assessed. However, the objectives of ITER must have been maintained. The reduction the size of the fusion reactor keeping the plasma performance is possible by increasing the plasma elongation. A simple estimate taking account the empirical scaling law of the plasma energy confinement shows that about 10% increase of the plasma elongation allows the reduction of the major radius by 0.4m. It is well-known that the increase of the elongation deteriorates the plasma vertical stability and may increase the cost for the power supply facilities. Therefore, the plasma position control occupied an important position in assessment of the sensitivity study.

This paper is a detailed summary of the plasma position control carried out by Japan ITER Home Team during the period of the sensitivity study in 1994. For the comprehensive summary of the plasma control in the sensitivity study, confer the document for the sixth meeting of the Technical Advisory Committee entitled 'Findings of the ITER sensitivity study'[3].

In next section, the analysis of the eddy current in the passive structures and the formulation to describe the motion of the plasma are given. In section 3, we show our model of the passive structure around the plasma. In section 4, we present the results of the plasma control simulations when finite horizontal disturbance fields are applied to the plasma. Section 5 summarizes the simulations when the disturbance field is small and the motion of the plasma is governed by the passive structures. Section 6 is used to show the simulations of the plasma motion when sudden changes of the poloidal beta(β_p) and the internal inductance(ℓ_i) occurs. The summary and discussions are given in section 7. The models of the plasma and passive structures used in the following analysis are the Outline Design and the elongated plasma, the Case (E), considered in the sensitivity study of ITER EDA. In Appendix, the derivation of the contribution due to the change of the plasma current profile is described.

2. The method of the analysis

2-1. The model of the passive structures around the plasma

The eddy current in the passive structures around the plasma plays an important role in controlling the plasma. The precise modeling of the blanket and the vacuum vessel is required. In our analysis, the finite element model was used. Among the methods to reproduce the effect of the passive structures, the finite element model is considered to be the most faithful to the design as long as the model is made properly.

Fig.1 is the finite element model used for the analysis of the eddy current. From inside, the elements are the first wall(FW), the back plate(BP), the inner wall of the vacuum vessel(V.V.) and the outer wall of the vacuum vessel. The 144-times discrete rotational symmetry in toroidal direction is assumed. The thickness of the wall is determined by the one-turn resistivity. In the analysis the thickness of the wall is assumed to be small compared with the skin effect and the current flow perpendicular to the surface is neglected. Therefore, the eddy current is assumed to flow in the surface of the wall. In order to formulate the eddy current, the current potential V_α is defined on each mesh point, where the index α stands for the mesh point. Then the eddy current is given by

$$\vec{j} = \vec{\nabla} V_\alpha \times \vec{n} \quad , \tag{1}$$

where the vector $\vec{n}$ is a normal unit vector of the surface.

For example, the circuit equations of the coils and the eddy currents are given in terms of the current potential,

$$\begin{aligned} &\partial_t\left(\sum_j M_{i,j} I_j\right) + \partial_t\left(\sum_\beta \overline{M}^V_{i,\beta} V_\beta\right) + \eta_i I_i = V_i \\ &\partial_t\left(\sum_j \overline{M}^V_{j,\alpha} I_j\right) + \partial_t\left(\sum_\beta M^V_{\alpha,\beta} V_\beta\right) + \Sigma_\beta R^V_{\alpha,\beta} V_\beta = 0 \end{aligned} \quad , \tag{2}$$

where M^V and R^V are inductance matrix and the resistance matrix when the current potential is used. On the right hand side of the first equation, V_i is the voltage applied externally to the i-th

coil. There exists a matrix E such that M^V and R^V are diagonalized simultaneously,

$$E^t \cdot M^V \cdot E = D_{diag} \quad , \qquad E^t \cdot R^V \cdot E = 1 \quad . \tag{3}$$

Using E and changing the base by $V_\alpha = (E \cdot X)_\alpha$, Eqs.(2) are written as

$$\begin{aligned} &\partial_t\left(\Sigma_j M_{i,j}\, I_j\right) + \partial_t\left(\Sigma_\beta G_{i,\beta}\, X_\beta\right) + \eta_i\, I_i = V_i \\ &\partial_t\left(\Sigma_j G_{j,\alpha}\, I_j\right) + \partial_t\left(D_\alpha\, X_\alpha\right) + X_\alpha = 0 \end{aligned} \tag{4}$$

where the matrix G is defined by

$$G_{i,\beta} \equiv \Sigma_\alpha\, \overline{M}^V_{j,\alpha}\, E_{\alpha,\beta} \quad , \tag{5}$$

where the Greek index of G is used to indicate the eigen mode of the eddy current. Similarly we define the plasma-eddy mode coupling by $G_{p,\beta}$. In the same manner, the plasma-eddy couplings are used to derive the circuit equation and the equation of motion of the plasma.

2-2. The linearized equations of the motion of the plasma

In describing the motion of the plasma, we use the rigid model, in which we assume that the shape of the plasma does not change during the its motion. In order to investigate the effect of the change in the internal inductance of the plasma, the formulation is presented in section 2-3. Unless it is mentioned, we assume that the plasma current profile is fixed during time evolution.

In deriving the equation of the motion of the plasma, we assume the toroidally symmetric motion of the plasma and we simulate the vertical(Z) and horizontal(R) motion of the plasma. The equations of motion of the plasma in Z and R directions are given by[4,5]

$$M_p \ddot{Z}_p = -\int drdz\, 2\pi R\, i_{p(r,z)}\, B_{R(r,z)}$$
$$M_p \ddot{R}_p = \frac{1}{2}\mu_0 I_p^2 \left\{ \ln\left(\frac{8R_p}{a_p}\right) + \beta_p + \frac{1}{2}(\ell_i - 3) \right\} + \int drdz\, 2\pi R\, i_{p(r,z)}\, B_{Z(r,z)} \quad , \qquad (6)$$

where dots on the left hand side mean the time derivatives and the first term on the right hand side in the second equation is the expansion force of the plasma. β_p is the poloidal beta and ℓ_i is the internal inductance of the plasma defined by

$$\beta_p = \frac{\bar{p}}{B_a^2/2\mu_0}, \qquad \ell_i = \frac{\int drdz\, B_p^2}{\pi a_p^2 B_a^2} \quad , \qquad (7)$$

where $\bar{p}$ is the volume averaged plasma pressure and B_a is an average poloidal field in the separatrix. B_R, B_Z in Eq.(6) are magnetic fields applied to the plasma externally.

Let us consider the case in which the plasma current profile and the shape is fixed. Expanding the equation of motion in Eqs.(6) with respect to the small shifts of the plasma position $(\delta Z, \delta R)$, we obtain linearized equations(cf. Appendix)

$$M_p \delta\ddot{Z}/I_p = 2\pi B_{vo} n \delta Z - 2\pi B_{vo} k \delta R + \sum_i^{coil} \frac{\partial M_{pi}}{\partial Z_p} I_i + \sum_k^{eddy} \frac{\partial G_{pk}}{\partial Z_p} X_k - 2\pi R_p B_{dR}$$
$$M_p \delta\ddot{R}/I_p = -2\pi B_{vo} k \delta Z + a_{22} \delta R + \left[-2\pi R_p B_{vo} - \mu_0 \beta_p I_p\right] \delta I_p / I_p \quad , \qquad (8)$$
$$+ \frac{1}{2}\mu_0 I_p \delta\beta_p + \sum_i^{coil} \frac{\partial M_{pi}}{\partial R_p} I_i + \sum_k^{eddy} \frac{\partial G_{pk}}{\partial R_p} X_k + 2\pi R_p B_{dZ}$$

where a_{22} is defined by

$$a_{22} = 2\pi B_{vo}\left(1 - n - \frac{1}{\Lambda_0}\right) - \frac{\mu_0 I_p}{4R_p} + \frac{1-2\gamma}{2R_p}\mu_0 I_p \beta_p \quad . \qquad (9)$$
$$\Lambda_0 = -4\pi R_p B_{vo}/\mu_0 I_p$$

The index γ is $\gamma = 5/3$. B_{dZ} and B_{dR} are vertical and horizontal disturbance fields. The adiabatic compression/decompression and the conservation of the toroidal flux in the plasma are assumed in Eqs.(8). The quantities n, k are indices which are the measures of the vertical stability and the coupling between the vertical

and horizontal motion respectively

$$n \equiv -\frac{1}{I_p B_{vo}} \int dr dz\, r\, i_{p(r,z)} \frac{\partial B_{z(r,z)}}{\partial r}$$
$$k \equiv -\frac{1}{I_p B_{vo}} \int dr dz\, r\, i_{p(r,z)} \frac{\partial B_{z(r,z)}}{\partial z} \quad , \tag{10}$$

and B_{vo} is the vertical field applied to the plasma

$$B_{vo} \equiv \frac{1}{I_p} \int dr dz\, i_{p(r,z)}\, B_{z(r,z)} \quad . \tag{11}$$

In deriving Eqs.(8), the vertical and horizontal balances in the equilibrium are used

$$\int dr dz\, r\, i_{p(r,z)}\, B_{R(r,z)} = 0$$
$$\frac{1}{2}\mu_0 I_p^2 \left\{ \ln\left(\frac{8R_p}{a_p}\right) + \beta_p + \frac{1}{2}(\ell_i - 3) \right\} + 2\pi I_p R_p B_{vo} = 0 \quad . \tag{12}$$

The circuit equations of the plasma, coils and eddy modes are given by

$$\partial_t\left(L_p I_p\right) + \sum_i^{coil} \partial_t\left(M_{p,i} I_i\right) + \sum_\alpha^{eddy} \partial_t\left(G_{p,\alpha} X_\alpha\right) + \eta_p I_p = 0$$
$$L_i\, \partial_t(I_i) + \partial_t\left(M_{p,i} I_i\right) + \sum_j^{coil} \partial_t\left(M_{i,j} I_j\right) + \sum_\alpha^{eddy} \partial_t\left(G_{i,\alpha} X_\alpha\right) + \eta_i I_i = V_i \quad , \tag{13}$$
$$\partial_t\left(G_{p,\alpha} I_p\right) + \sum_i^{coil} \partial_t\left(G_{i,\alpha} I_i\right) + D_\alpha \partial_t\left(X_\alpha\right) + X_\alpha = 0$$

where index p stands for the plasma. Assuming that the eddy eigen mode X_α is the first-order small quantity and expanding the plasma current and coil currents into the equilibrium values and the shifts from them

$$I_p \to I_p + \delta I_p \,, \qquad I_i \to I_i + \delta I_i \quad ,$$

the linearized equations of Eqs.(13) become

$$
\begin{aligned}
&-\left(2\pi R_p+\mu_0 I_p \beta_p\right)\delta\dot{R}_p + I_p L_p\left(\delta\dot{I}_p/I_p\right) \\
&\qquad +\sum_j^{coil} I_p M_{p,j}\left(\delta\dot{I}_j/I_p\right)+\sum_\alpha^{eddy} I_p G_{p,\alpha}\left(\dot{X}_\alpha/I_p\right)+\eta_p I_p\left(\delta I_p/I_p\right)=0 \\
&\left(\frac{\partial M_{p,i}}{\partial Z_p}I_p\right)\delta\dot{Z}_p+\left(\frac{\partial M_{p,i}}{\partial R_p}I_p\right)\delta\dot{R}_p+I_p M_{p,i}\left(\delta\dot{I}_p/I_p\right)+I_p L_i\left(\delta\dot{I}_i/I_p\right) \\
&\qquad +\sum_j^{coil} I_p M_{i,j}\left(\delta\dot{I}_j/I_p\right)+\sum_\alpha^{eddy} I_p G_{i,\alpha}\left(\dot{X}_\alpha/I_p\right)+\eta_i I_p\left(\delta I_i/I_p\right)=V_i \quad . \qquad (14) \\
&\left(\frac{\partial G_{p,\alpha}}{\partial Z_p}I_p\right)\delta\dot{Z}_p+\left(\frac{\partial G_{p,\alpha}}{\partial R_p}I_p\right)\delta\dot{R}_p+I_p G_{p,\alpha}\left(\delta\dot{I}_p/I_p\right) \\
&\qquad +\sum_j^{coil} I_p G_{\alpha,j}\left(\delta\dot{I}_j/I_p\right)+I_p D_\alpha\left(\dot{X}_\alpha/I_p\right)+I_p\left(X_\alpha/I_p\right)=0
\end{aligned}
$$

In deriving Eq.(14), the assumptions of the adiabatic motion of the plasma and the conservation of the toroidal flux are used. Neglecting the mass term of the plasma in Eqs.(8) and taking derivatives of them, we obtain the first order differential equations with respect to time.

It is convenient to write down the equations in a matrix form. Let us define a vector Y by

$$
Y={}^t\left(\delta Z,\delta R,\delta I_p/I_p,\cdots\delta I_i/I_p\cdots,\cdots X_\alpha/I_p\cdots\right) \quad .
$$

Then the sum of the equation of motion and the circuit equation is expressed as

$$
A\dot{Y}+RY=B \quad , \qquad (15)
$$

where A is a matrix defined by

$$A=\begin{pmatrix} 2\pi B_{vo} & -2\pi B_{vo}k & 0 & \cdots & I_p\partial_Z M_{p,i} & \cdots & \cdots & I_p\partial_Z G_{p,\alpha} & \cdots \\ -2\pi B_{vo}k & a_{2,2} & a_{2,3} & \cdots & I_p\partial_R M_{p,i} & \cdots & \cdots & I_p\partial_R G_{p,\alpha} & \cdots \\ 0 & a_{2,3} & I_p L_p & \cdots & I_p M_{p,i} & \cdots & \cdots & I_p G_{p,\alpha} & \cdots \\ \vdots & \vdots & \vdots & \ddots & & & & \vdots & \\ I_p\partial_Z M_{p,i} & I_p\partial_R M_{p,i} & I_p M_{p,i} & & I_p M_{i,j} & & \cdots & I_p G_{i,\alpha} & \cdots \\ \vdots & \vdots & \vdots & & & \ddots & & \vdots & \\ \vdots & \vdots & \vdots & & \vdots & & \ddots & & 0 \\ I_p\partial_Z G_{p,\alpha} & I_p\partial_R G_{p,\alpha} & I_p G_{p,\alpha} & \cdots & I_p G_{i,\alpha} & \cdots & & I_p D_\alpha & \\ \vdots & \vdots & \vdots & & \vdots & & 0 & & \ddots \end{pmatrix} \quad . \quad (16)$$

$$a_{2,3}=-\left(2\pi R_p+\mu_0 I_p \beta_p\right)$$

The diagonal matrix R and the vector B are given by

$$R_{diag}={}^t\left(0,0,I_p\eta_p,\cdots I_p\eta_i\cdots,\cdots I_p\cdots\right)$$
$$B={}^t\left(2\pi R_p\dot{B}_{dR},-2\pi R_p\dot{B}_{dZ}-\frac{1}{2}\mu_0 I_p\delta\dot{\beta}_p,0,\cdots V_i\cdots,\cdots 0\cdots\right) \quad . \quad (17)$$

In Eqs.(14) and (17), V_i is a voltage used to the plasma position control. Eqs.(15)-(17) are the equations to be solved. For the numerical computation, we used the 6-th order Fehlberg method.

2-3. The change of the plasma current profile

In the formulation in section 2-3, the plasma current profile is assumed to be fixed. However, in experiments it is known that the changes of the plasma current profile occur during MHD activities[6]. In this section, the equation Eq.(15) is modified so that the effect of the change of the plasma current profile is taken into account in the linearized approximation.

The change of the plasma current density is written by

$$i_p \rightarrow i_p+\delta i_p \quad .$$

We use the internal inductance defined in Eq.(7) to express the change of the plasma current profile. In this sense, we

concentrate on the change of the plasma current profile such that it is expressed by the global quantity ℓ_i . Assuming that the quantities associated with the change of the current profile are first order small quantities, the modification is obtained straightforwardly. The modification appears only in the vector B in Eqs.(15) and (17),

$$B=\begin{pmatrix} 2\pi R_p \dot{B}_{dR} - \partial_{\ell_i} F_Z \, \delta\dot{\ell}_i \\ -2\pi R_p \dot{B}_{dZ} - \mu_0 I_p \left(\delta\dot{\beta}_p + \delta\dot{\ell}_i/2\right)/2 - \partial_{\ell_i} F_R \, \delta\dot{\ell}_i \\ -\left(\partial_{\ell_i} L_p I_p + \sum_j^{coil} I_j \partial_{\ell_i} M_{p,j}\right)\delta\dot{\ell}_i \\ \vdots \\ V_i - \partial_{\ell_i} M_{p,i} I_p \, \delta\dot{\ell}_i \\ \vdots \\ -\partial_{\ell_i} G_{p,\alpha} I_p \, \delta\dot{\ell}_i \\ \vdots \end{pmatrix} , \tag{18}$$

where ∂_{ℓ_i} denotes the derivative with respect to the plasma internal inductance and I_j appearing in the third line of Eq.(18) is the coil current at the equilibrium. The quantities, $\partial_{\ell_i} F_Z$ and $\partial_{\ell_i} F_R$ are forces due to the equilibrium fields defined by

$$\begin{aligned} \partial_{\ell_i} F_Z &\equiv -\frac{1}{\delta\ell_i}\frac{2\pi}{I_p}\int drdz \, r \, \delta i_{p\,(r,z)} \, B_{R(r,z)} \\ \partial_{\ell_i} F_R &\equiv \frac{1}{\delta\ell_i}\frac{2\pi}{I_p}\int drdz \, r \, \delta i_{p\,(r,z)} \, B_{Z(r,z)} \end{aligned} , \tag{19}$$

where B_R, B_Z are magnetic fields in equilibrium. In deriving the derivatives with respect to ℓ_i , we use two plasma configuration with different plasma internal inductances and take the difference of them. The derivation of Eqs.(18) and (19) is described in Appendix.

It is not obvious how the fluctuations appear during experiments. Therefore we have to perform the parametric survey with respect the disturbance parameters. Such parameter survey was carried out and the results are summarized in sections 6.

2-4. The PDI plasma position control and simulation parameters

The PDI feedback control with respect to the displacements of the plasma positions is employed. Let us denote the vertical and horizontal position of the plasma from the equilibrium by δZ and δR , then the voltage applied to a coil for the feedback control is given by

$$V_{FB} = G_{Z,P}\left\{\delta Z + G_{Z,D}\frac{\partial \delta Z}{\partial t} + G_{Z,I}\int_{t_0}^{t} dt\,\delta Z\right\} + G_{R,P}\left\{\delta R + G_{R,D}\frac{\partial \delta R}{\partial t} + G_{R,I}\int_{t_0}^{t} dt\,\delta R\right\} , \quad (20)$$

where subindexes P, D, I means proportional, differential and integral, respectively. t_0 is the time when the control is active. In analysis of this paper, we use the differential and proportional controls and integral controls are not used.

In order to simulate the control system, we introduce following parameters.

(1) Sampling time: Every sampling time, the result of plasma position measurement is used to compute the feedback control voltage according to Eq.(20). The standard value we use in the analysis is 1 msec.

(2) Delay time of the diagnostics: It is assumed that there is a certain time delay to get the results of the plasma position in the diagnostic system. The standard value in the analysis is 1 msec.

(3) The condition of starting the control: Let us introduce Z_0 , R_0 such that the position control becomes active when $|\delta Z|$ exceeds Z_0 or $|\delta R|$ exceeds R_0 . The standard values of Z_0 , R_0 are 1 cm.

(4) The minimum recognizable fluctuation: The minimum fluctuations of the plasma position which is recognizable by the diagnostics are introduced. These values are basic in the feedback control. Although it is rather optimistic, we use 10^{-5}cm in simulations.

In the analysis, we assume that the motion of the plasma is initiated by the fluctuations. We consider three types of the

fluctuations, the horizontal field, the change of the poloidal beta value and the internal inductance of the plasma. For simulations, we have to give the time evolution of these fluctuations. Therefore, we introduce time constants τ and define the time evolutions. For example, the horizontal field fluctuation is given by

$$B_{R,d}(t) = B_{R,d,0}\left[1-\exp(-t/\tau)\right] \quad . \tag{21}$$

Those of the poloidal beta and the plasma internal inductance are given similarly.

As measures of the plasma controllability, we introduce two quantities, the settling time and overshooting for the vertical and horizontal motion. The settling time and overshooting of the vertical motion are defined by

$$\tau_{sett,Z} = \int_{t_0}^{\infty} dt|\delta Z| \Big/ |Z_0| \quad , \qquad Overshooting_Z = \left(|\delta Z|_{\max} - |Z_0|\right) \Big/ |\delta Z_0| \quad , \tag{22}$$

where Z_0 is the vertical fluctuation to start control and t_0 is the time the control becomes active. The settling time has a meaning equivalent to the decay time of the fluctuation when the overshooting is small.

3. The model of the passive structure and the evaluation of the plasma stabilization effect.

As we have mentioned in section 2, we use the finite element method to analyze the eddy currents on the passive structure around the plasma. FIG. 1 shows the mesh model used for our analysis in the case of the outline design of ITER EDA. The model consists of the vacuum vessel(V.V.), the back plate of the blanket(B.P.) and the first wall of the blanket(F.W.). In our model, the vacuum vessel has a double-wall structure. The one-turn resistivity of each components are:

Vacuum Vessel :	26 μΩ
Back Plate :	16 μΩ
First Wall :	100 μΩ .

The model for the case(E) is basically the same as that in FIG.1, except small modifications of the size.

In order to evaluate the plasma stabilization effect of the passive structures, we perform the Laplace analysis of the linearized equation. The γ－Laplace component of the shell stabilization index, $n_{(\gamma)}$, is defined by

$$n_{(\gamma)} = -\frac{\gamma}{2\pi B_{v0}} I_p \,{}^t\!\left(A^Z\right) \tilde{M}^{-1} \left(A^Z\right)$$

$$\tilde{M} = \begin{bmatrix} \gamma M_{i,j} + \eta_i \delta_{i,j} & \gamma G_{\alpha,i} \\ \gamma G_{\alpha,j} & (1+\gamma D_\alpha)\delta_{\alpha,\beta} \end{bmatrix}, \qquad A^Z = \begin{bmatrix} \langle \partial_{Z_r} M_{p,i} \rangle \\ \langle \partial_{Z_r} G_{p,\alpha} \rangle \end{bmatrix} .$$

The above equation includes effects of eddy currents on the passive structures and passive coils. Then, the condition of the stabilization is given by

$$n + n_{(\gamma)} > 0 \quad ,$$

where n is the index defined in Eq.(10).

FIG.2 is the result of the vertical stabilization effects of the passive structures for the Outline Design (FIG.2-1) and the

Case (E) (FIG.2-2). The numbers in these figures are the quantities obtained by the equilibrium analysis. The horizontal dotted line in figures indicates the value of n-index. The growth rate of the outline design and the Case(E) are:

Outline Design : 1.2 (1/sec)
Case (E) : 3.0 (1/sec) .

The elongation of the case(E) is bigger than that of the outline design. As a result, the growth rate of the case(E) is bigger than the outline design.

For the fast motion of the plasma, the poloidal field(PF) coils play roles of the passive structures. Therefore, the effect of PF coils to the plasma stabilization effect is also evaluated. In the outline design, the analysis including the PF coils gives the growth rate about 1 (1/sec). Thus we can estimate that about 20% of improvement is expected when the passive effect of the PF coils are taken into account.

4. The simulation study I

(Simulations when finite horizontal disturbance fields are applied)

The plasma shows various behaviors depending on fluctuations applied to the plasma. This section is a summary of the simulation study investigating the cases when horizontal fluctuation fields are applied. The origins of such fluctuations in reality are an accident of the coils and the sudden change of the plasma current profile so that the plasma feels an effective horizontal field. ITER EDA has 7 PF coils. Among them, we use outer PF coils for control. FIG.3 show the positions of the PF coils and other structures for the outline design. In this section, we show results using PF2, 3, 5, 7 for the control. However, we checked the control using all 6 outer coils and found only small differences.

For comparison between different elongations, we use the outline design(OD) and the elongated plasma, the case(E), considered in the sensitivity study. The main parameters of these plasmas are summarized in table 1.

	Outline Design	Case (E)
Major radius (m)	8.1	7.5
Minor radius (m)	3.0	2.78
Toroidal field (T)	5.72	5.2
Plasma current (MA)	24	23.3
Elongation(95%)	1.55	1.7
Poloidal beta	0.7	0.7
Internal inductance	0.9	0.9

TABLE 1, Major parameters of the Outline Design and Case (E) of ITER EDA.

The case(E) has the same number of PF coils and their positions are determined according to its radial build. We use the same numbering as the outline design to denote the PF coils of case(E).

4-1. The dependence on the control voltage

The control simulations of OD and E plasmas for different voltage limits of PF coils are summarized in FIG.4. The horizontal fluctuation field is 5G with time constant 1 msec and the control is initiated by detecting 1cm of vertical fluctuation ($Z_0 = 1cm$). PF coils #2, 3, 5, 7 in FIG.3 are used for the control. FIG.4-1 shows the settling time of the vertical motion and FIG.4-2 is the overshooting. In these simulations, the same gains of the PD feedback control in Eq.(20) are assigned to the PF coils except the signs of the proportional gains. We define the optimum control by those which give the minimum settling times. The results in FIG.4 are obtained by the control gains which minimize the settling times.

As representative simulations, FIG.5 shows the time evolution of the plasma control of the outline design when the control voltage limit is 3V. FIG.5-1 is the vertical and horizontal fluctuations and FIG.5-2 is the plasma current fluctuation normalized by the plasma current in the equilibrium. FIGs.5-3 to 5-6 are the voltages and currents of PF coils. The voltages and currents in these figures are in one-turn and we shall stress that there are equilibrium currents of PF coils which are not added in figures. FIG.6 is the simulation of case(E) when the horizontal fluctuation field is 5G and the voltage limit is 5V. The results in FIGs.5 and 6 are moderate simulations in the sense that the voltage applied to PF coils are not changing rapidly in time. However, for controls of small voltage limits, the applied voltages and consequent coil currents become bumpy and they are not adequate for the control.

4-2. The dependence on the horizontal fluctuation field

The behaviors of the plasma depend on the fluctuations applied to the plasma. In this section, we observe the motion of plasma when the horizontal fluctuation fields is applied to the plasma. If the fluctuation field is small such that the effect of

the fluctuation field to the motion of the plasma is neglected, the motion of the plasma is governed by the characteristics of the passive structures around the plasma. Detailed study of such cases are discussed in section 5. In section 4-2, we summarize dependences on the horizontal fields when the fluctuation field is finite.

FIG.7 is the summary of the simulations as the horizontal fluctuation field is changed. The plasma is the outline design in table 1 and $Z_0 = 1cm$. The voltage limits of PF coils used for the control are 7V and 5V. The control gains are optimized at each point. FIG.7-1 shows the settling time and FIG.7-2 the overshooting of the vertical motion. There is a tendency that the control becomes worse rapidly as the increase of the fluctuation field. FIG.8 is the time evolution of the vertical and horizontal motion of the plasma for the fluctuation field 5G(FIG.8-1) and 20G(FIG.8-2) when the control voltages are limited under 5V.

4-3. The simulations of plasmas with different β_p

It is known that the vertical position control becomes more difficult as the poloidal beta decreases and the internal inductance increases. The value of the poloidal beta at the flat top is 0.7. FIGs.9 and 10 are comparisons of the simulations in the cases poloidal beta 0.1 and 0.7. for the outline design(FIG.9) and case(E)(FIG.10). There is not big difference between the simulations of the plasma with the small poloidal beta and the normal plasma. This is due to the small value of the horizontal fluctuation field used for the simulation. The difference between the a small poloidal beta and the normal poloidal beta becomes clear when the fluctuation field is large.

4-4. The dependence on the condition to initiate the control

In the previous sections, the feedback control is initiated by detecting 1cm of the plasma displacement. However, this condition depends on the design of the passive structures and the diagnostics. Therefore it is appropriate to understand the dependence of the plasma control on the condition to initiate the feedback control. In order to estimate this dependence, the simulations which apply constant control voltages when the displacement Z_0 is detected are carried out and dependence on Z_0 is investigated. FIG.11 is the time evolutions of the vertical displacements for the outline design plasma and $\delta B_r = 5G$. FIG.11-1 shows the results for $Z_0 = 1cm$ and FIG.11-2 $Z_0 = 10cm$. The feedback control is not used for these simulations. Thus the voltages in FIGs. imply those which push back the plasma in the positive-Z direction. FIGs.11 show that at least 0.65V is need to push the plasma back to positive-Z for $Z_0 = 1cm$ and 2.7V for $Z_0 = 10cm$. There fore, about a factor of 4 increase of the control voltage is expected when the feedback control is initiated by detecting 10cm displacement compared with the one by detecting 1cm displacement.

FIG.12 is the results of the same analysis for the case (E). Since the elongation of Case (E) plasma is larger than the outline design plasma, the vertical position control is more severe. FIG.12 shows that more than a factor of 5 increase of the control voltage is needed when 10cm plasma displacement is used to start control compared with that of 1cm.

5. The simulation study II

(Simulations when the motion of the plasma is governed by the passive structures)

As we have discussed in section 4-2, the motion of the plasma depends on the disturbance applied to the plasma. When the disturbance is small, the motion of the plasma is governed by passive structures around the plasma, namely the blanket and vacuum vessel. Then the characteristic time of the motion of the plasma is determined by the growth rate of the passive structures shown in FIG.2.

Similar analysis as those in FIGs.11 and 12 have been carried out for smaller horizontal disturbance fields, i.e. $\delta B_r \geq 0.1G$ in stead of 5G. The results are summarized in FIGs.13-1 and 13-2 for the outline design and case(E). The vertical axis in FIG.13 is the voltage of the control coils when the overshooting equals to 1. We found that when the horizontal fluctuation field is about 0.2G the plasma vertical displacement grows with the growth rate obtained by FIG.2. Therefore, when the horizontal fluctuation is 0.2G or smaller than that, the plasma motion is governed by the characteristics of the passive structures. The fluctuation field is used just to initiate the motion of the plasma and does not affect the evolution.

The PD feedback controls are simulated by applying the horizontal fluctuation field 0.2G. The dependences of the settling time and the overshooting of the vertical motion on the applied voltages are summarized in FIG.14. Because of the higher elongation, larger control voltages are required for the control of the case(E) plasma. The plasma position controls become severer rapidly as the decrease of the voltage limit used for control. It seems that there exists limits of controllable voltages at about 0.4V for the outline design and 1.5V for the case(E). FIG.15 shows the time evolutions of the plasma control of the outline design when the voltage limit of coils are 0.5V. FIG.15-1 is the vertical and horizontal fluctuations and FIG.15-2 is the plasma current fluctuation normalized by the plasma current in the equilibrium. FIGs.15-3 to 15-6 are the voltages and currents of PF coils. Similarly, FIG.16 is the time evolution of

the plasma control for the case(E) when 2V is allowed.

6. The simulation study III

(Simulations when sudden β_p, ℓ_i changes occur)

During discharges of the fusion experiments, the fluctuations of the poloidal beta and internal inductance occur because of MHD activities. In the analysis of the sensitivity study, it is considered that at least the motion of the plasma due to 0.2 drop of the poloidal beta should be controlled. In the linearized formulation, the effects of β_p, ℓ_i changes are formulated in sections 2-2 and 2-3. In section 2-3, the change of the internal inductance is assumed to be due to the variation of the plasma current profile. Since there are possibilities of both increasing and decreasing the internal inductance, we perform the parametric survey of the motion of the plasma with respect to the change of the internal inductance.

FIG.17 is the motion of the plasma when -0.2 drop of the poloidal beta and the increase of the internal inductance(peeking of the plasma current profile) occurs. FIG.17-1 is the vertical motion and FIG.17-2 is the horizontal motion. In these simulations, no feedback control is used. The time variation of $\delta\beta_p, \delta\ell_i$ are given similarly to Eq.(21). Their time constants used in FIG.17 are 1 msec for the poloidal and 10 msec for the internal inductance. FIG.17 shows that the vertical displacement increases as an increase of the internal inductance. This is because the plasma feels an effective negative horizontal field due to the peeking of the plasma current profile. The horizontal motion is understood as a consequence of the Shafranov term in Eq.(6). FIG.18 is the simulation when the drop of the internal inductance happens.

FIG.19 shows the dependences of the plasma motion on the time constant of the increase of the internal inductance. The internal inductance is increase by 0.1 and the change of the poloidal beta

the plasma control for the case(E) when 2V is allowed.

6. The simulation study III

(Simulations when sudden β_p, ℓ_i changes occur)

During discharges of the fusion experiments, the fluctuations of the poloidal beta and internal inductance occur because of MHD activities. In the analysis of the sensitivity study, it is considered that at least the motion of the plasma due to 0.2 drop of the poloidal beta should be controlled. In the linearized formulation, the effects of β_p, ℓ_i changes are formulated in sections 2-2 and 2-3. In section 2-3, the change of the internal inductance is assumed to be due to the variation of the plasma current profile. Since there are possibilities of both increasing and decreasing the internal inductance, we perform the parametric survey of the motion of the plasma with respect to the change of the internal inductance.

FIG.17 is the motion of the plasma when －0.2 drop of the poloidal beta and the increase of the internal inductance(peeking of the plasma current profile) occurs. FIG.17-1 is the vertical motion and FIG.17-2 is the horizontal motion. In these simulations, no feedback control is used. The time variation of $\delta\beta_p, \delta\ell_i$ are given similarly to Eq.(21). Their time constants used in FIG.17 are 1 msec for the poloidal and 10 msec for the internal inductance. FIG.17 shows that the vertical displacement increases as an increase of the internal inductance. This is because the plasma feels an effective negative horizontal field due to the peeking of the plasma current profile. The horizontal motion is understood as a consequence of the Shafranov term in Eq.(6). FIG.18 is the simulation when the drop of the internal inductance happens.

FIG.19 shows the dependences of the plasma motion on the time constant of the increase of the internal inductance. The internal inductance is increase by 0.1 and the change of the poloidal beta

is fixed to $\delta\beta_p = -0.2, \tau_{\beta_p} = 1msec$. Similarly, FIG.20 is the results when drops of the internal inductance occur. The initial motion is determined by the fluctuation with a smaller time constant, but a larger fluctuation governs the motion of the plasma in a long time scale. As one sees in FIGs.17-20, the change of the internal inductance poses more serious demands. Especially when the vertical and horizontal motion interacts each other to worsen the plasma fluctuations, the plasma control becomes severe.

The outline design plasma has no instability in the horizontal motion. Therefore, the priority must be payed to control the vertical motion first and the horizontal position is shifted appropriately afterward. FIG.21 is an example of PD control when 10% drops of the poloidal beta and internal inductance occur simultaneously in 10 msec. The control voltages are limited under 10V. All PF coils are used to control the plasma, although CS coil is not effective to the vertical control. The vertical and horizontal gains are:

$$Z: \ G_{Z,D} = 1.0, G_{Z,P} = \pm 1000, \qquad R: \ G_{R,D} = 0.3, G_{R,P} = \pm 500 \quad ,$$

where the signs of the proportional gains depend on the position of the coils. Because of k-index in Eq.(6), the vertical and horizontal motions couple each other and this effect makes the control more difficult in the case of FIG.21. The detailed study on the controls when the changes of both the poloidal beta and internal inductance appear simultaneously should be done in the future work.

7. Summary and discussion

In this paper, the analysis of the plasma position control using the model described in section 2 is presented. Let us summarize the results. The requirement of the control system depends on the perturbations of the plasma which the system have to stabilize. About 3-5V of control voltage provides a

is fixed to $\delta\beta_p = -0.2, \tau_{\beta_p} = 1 msec$. Similarly, FIG.20 is the results when drops of the internal inductance occur. The initial motion is determined by the fluctuation with a smaller time constant, but a larger fluctuation governs the motion of the plasma in a long time scale. As one sees in FIGs.17-20, the change of the internal inductance poses more serious demands. Especially when the vertical and horizontal motion interacts each other to worsen the plasma fluctuations, the plasma control becomes severe.

The outline design plasma has no instability in the horizontal motion. Therefore, the priority must be payed to control the vertical motion first and the horizontal position is shifted appropriately afterward. FIG.21 is an example of PD control when 10% drops of the poloidal beta and internal inductance occur simultaneously in 10 msec. The control voltages are limited under 10V. All PF coils are used to control the plasma, although CS coil is not effective to the vertical control. The vertical and horizontal gains are:

$$Z: \ G_{Z,D} = 1.0, G_{Z,P} = \pm 1000, \qquad R: \ G_{R,D} = 0.3, G_{R,P} = \pm 500 \quad ,$$

where the signs of the proportional gains depend on the position of the coils. Because of k-index in Eq.(6), the vertical and horizontal motions couple each other and this effect makes the control more difficult in the case of FIG.21. The detailed study on the controls when the changes of both the poloidal beta and internal inductance appear simultaneously should be done in the future work.

7. Summary and discussion

In this paper, the analysis of the plasma position control using the model described in section 2 is presented. Let us summarize the results. The requirement of the control system depends on the perturbations of the plasma which the system have to stabilize. About 3-5V of control voltage provides a

satisfactory controllability of ITER EDA plasma when disturbances equivalent to 5-10G of the horizontal field are considered. For the control of plasma moving in the characteristic time of the passive structures, a few volt of the control voltage is enough. The control of the plasma, when the changes of the poloidal beta and internal inductance occur, is demanding especially in the case that the vertical and horizontal motions interact to increase their displacements each other. The study on such controls has yet to be done.

Our model assume that the shape of the plasma does not change during the evolution. Such models are called as a rigid model due to their assumption. The rigid model has an ability to simulate the small motion of the plasma, however the approximation becomes worse as the fluctuation grows. Therefore in order to simulate plasmas in critical situations, for example the plasma moves very close to the first wall, the model in which the change of the plasma shape is taken into account should be used.

It is difficult to justify if the control system is robust enough to stabilize the plasma against various kinds of instabilities. As we have discussed in previous sections, the requirement on the control system differs according to instabilities the system is subject to control. Thus, it is important to determine to what extent the stabilization capacity should be prepared. It is also important how to quantify the controllability and compare the controls. For example, if one compares the simulations of the outline design and case(E) with the same settling time, one concludes that about a factor 2 of voltage is needed to control the plasma of case(E) compared with the outline design. However, if one compares simulation with the same overshooting, the factor is about 3.

Among the simulations discussed above, the controls of plasma when the changes of the poloidal beta and internal inductance occur give the severest requirement on the control capacity. This is because of the coupling between the vertical and horizontal motion, which is characteristic to the up-down asymmetric plasma. The detailed study is now under way. The preliminary results show that a large control voltages are needed to control about 10% drops of the poloidal beta and internal inductance.

REFERENCES

[1] ITER physics, ITER Document series No.21.

[2] ITER Outline Design Report,(ITER TAC-4-01, January 1994).

[3] Findings of the ITER Sensitivity Study,(ITER TAC-6-01, July 1994).

[4] M. Kasai, A. Kameari, F. Matsuoka, K. Shinya, H. Iida and N. Fujisawa, Fusion Engrg. Des., 5 (1988) 343.

[5] S. Nishio, M. Sugihara and Y. Shimomura,Fusion Engrg. Des., 23 (1993) 17.

[6] O. Gruber, K. Lackner, G. Pautasso, U. Seidel, B. Streibl, Plasma Phys. Control Fusion 35 (1993) B191-B204.

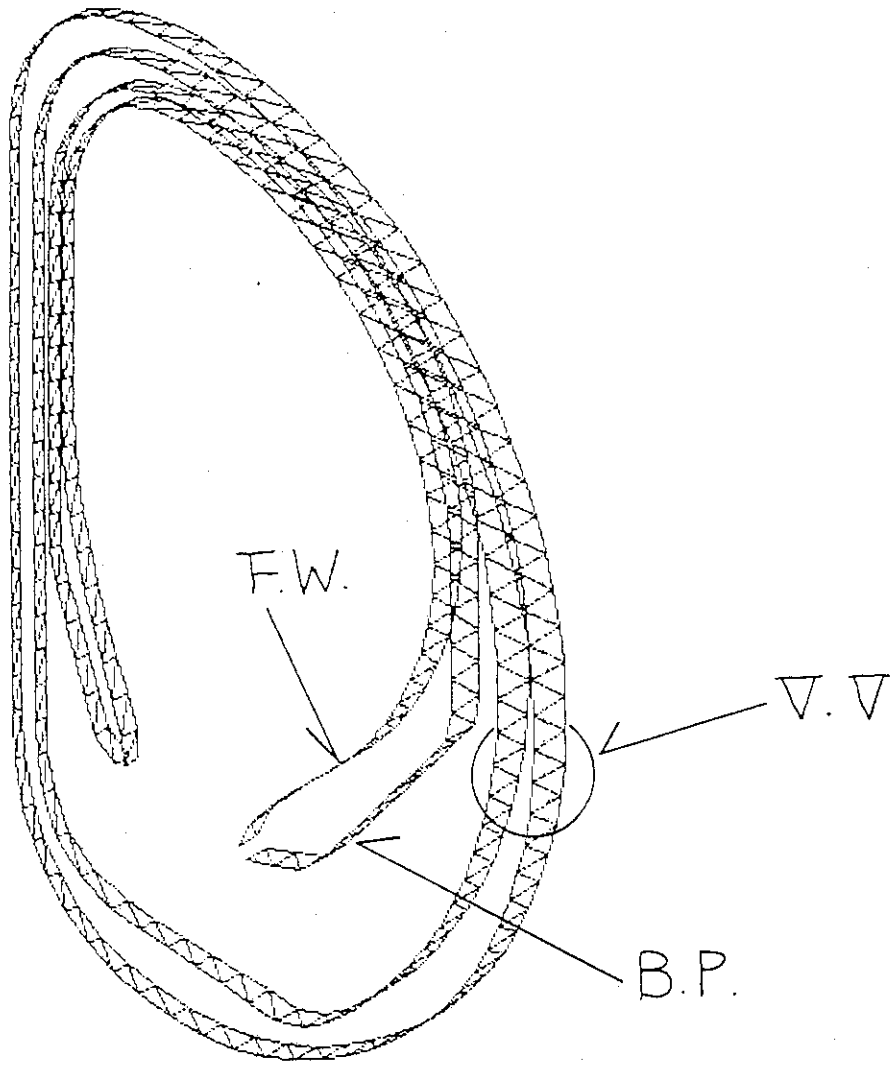

Fig. 1 The model of passive structure around the plasma

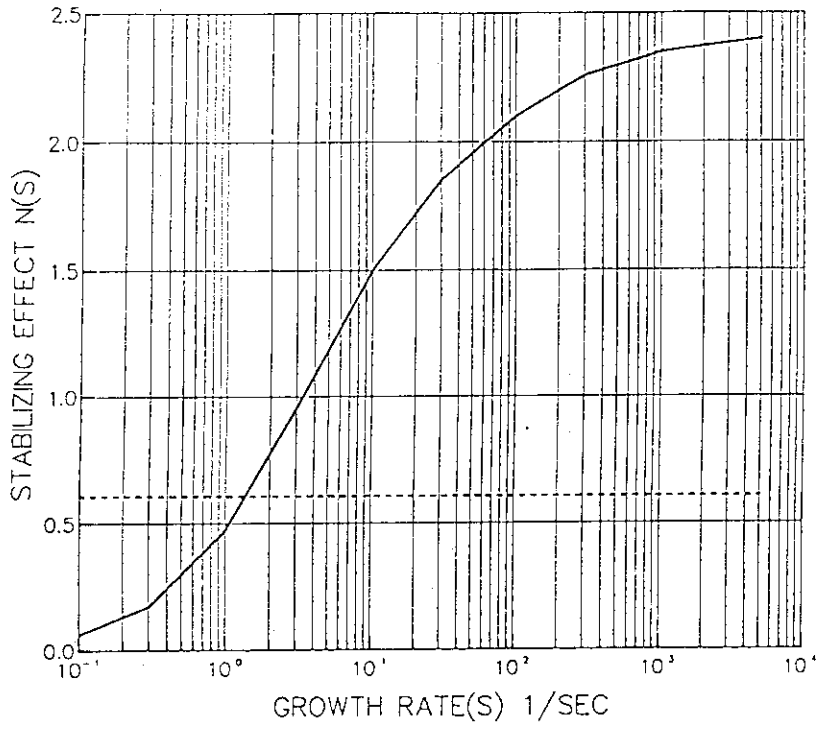

Fig. 2-1 The plasma stabilization effect in Outline Design

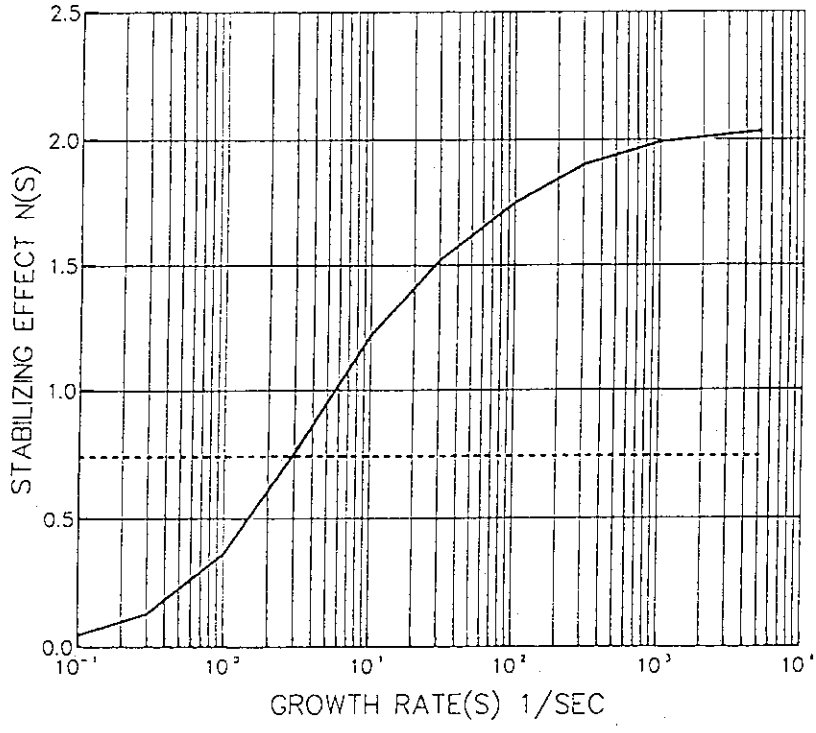

Fig. 2-2 The plasma stabilization effect in Case (E)

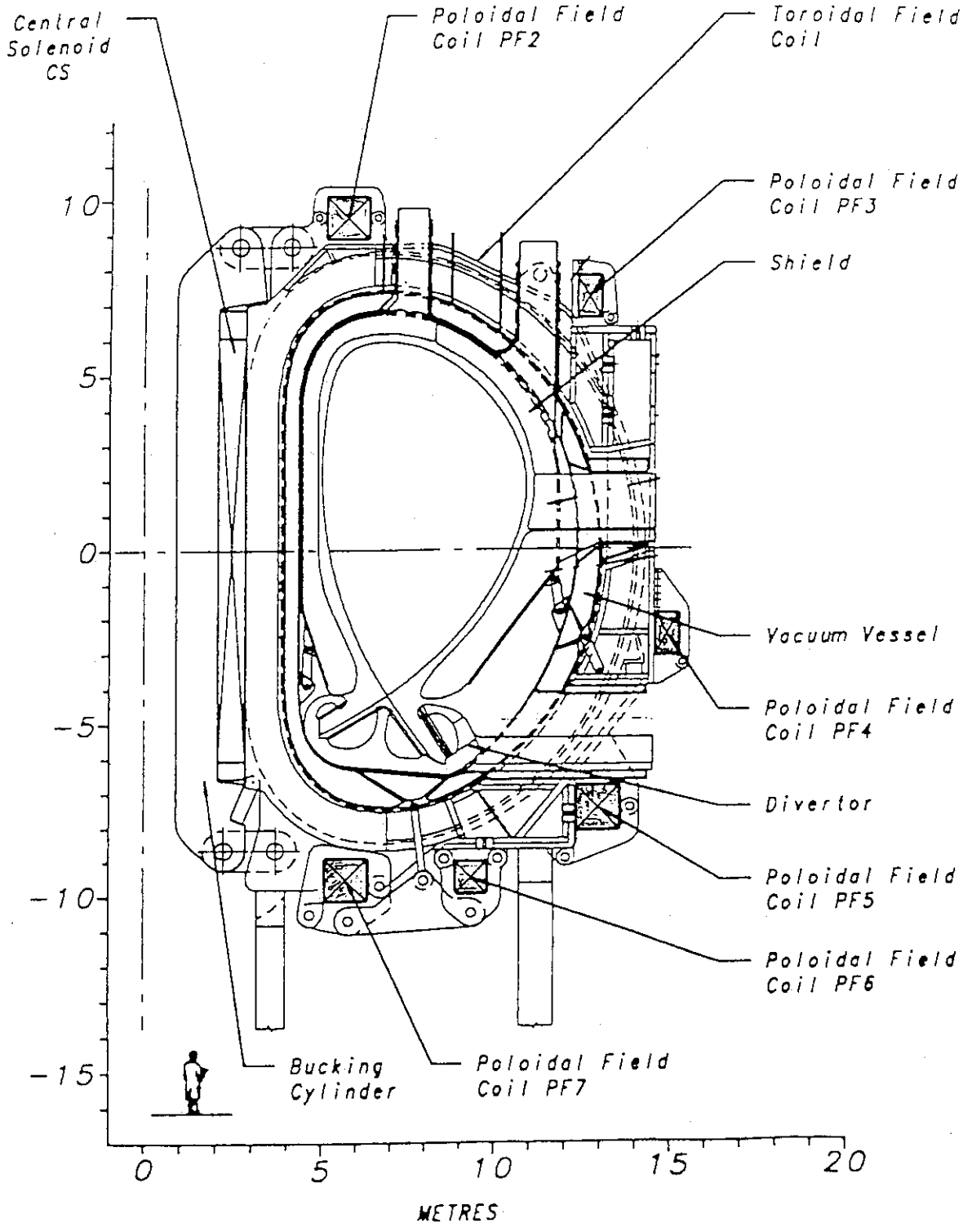

Fig. 3 The positions of PF coils

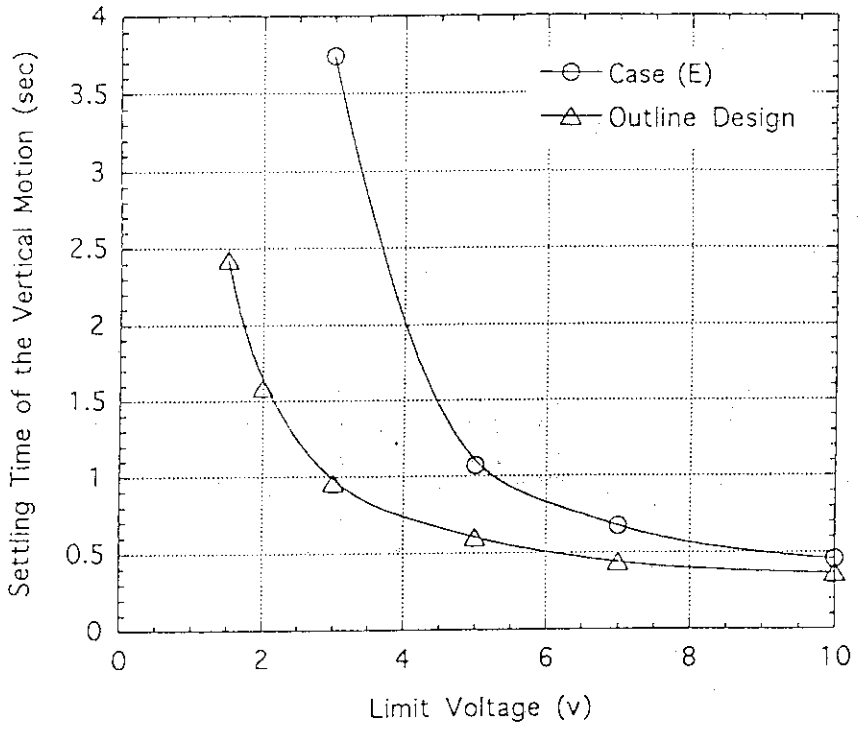

Fig. 4-1 Settling time vs. Voltage limit for $\delta B_r = 5\,G$

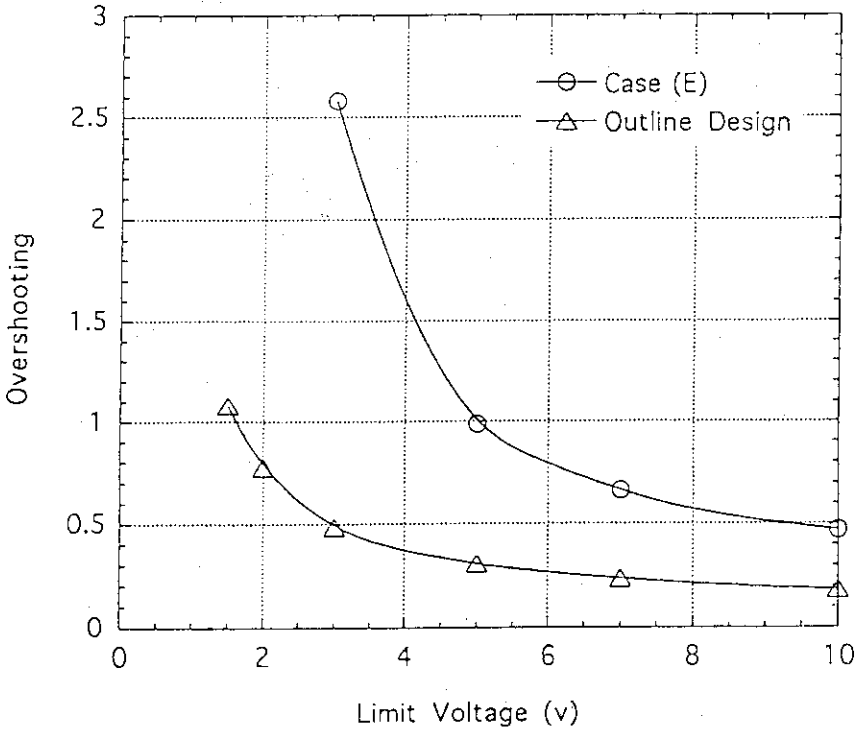

Fig. 4-2 Overshooting vs. Voltage limit for $\delta B_r = 5\,G$

Fig. 4 Simulation results in the case $\delta B_r = 5\,G$, $Z_0 = 1\,cm$

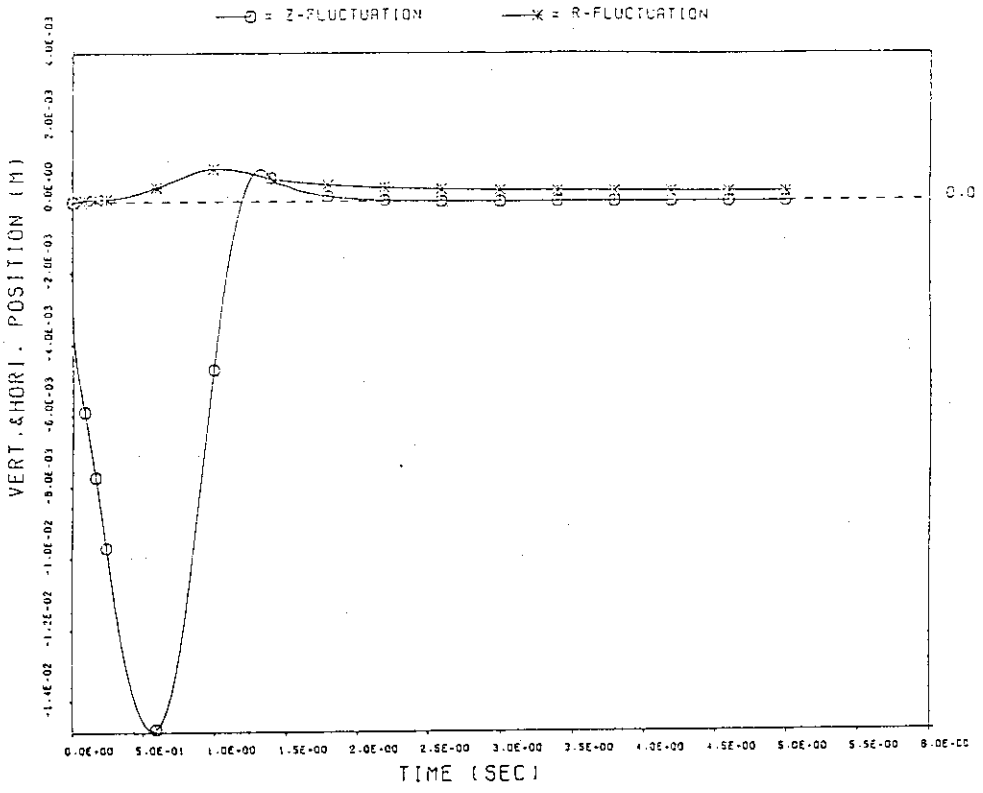

Fig. 5-1 Vertical and Horizontal plasma fluctuations

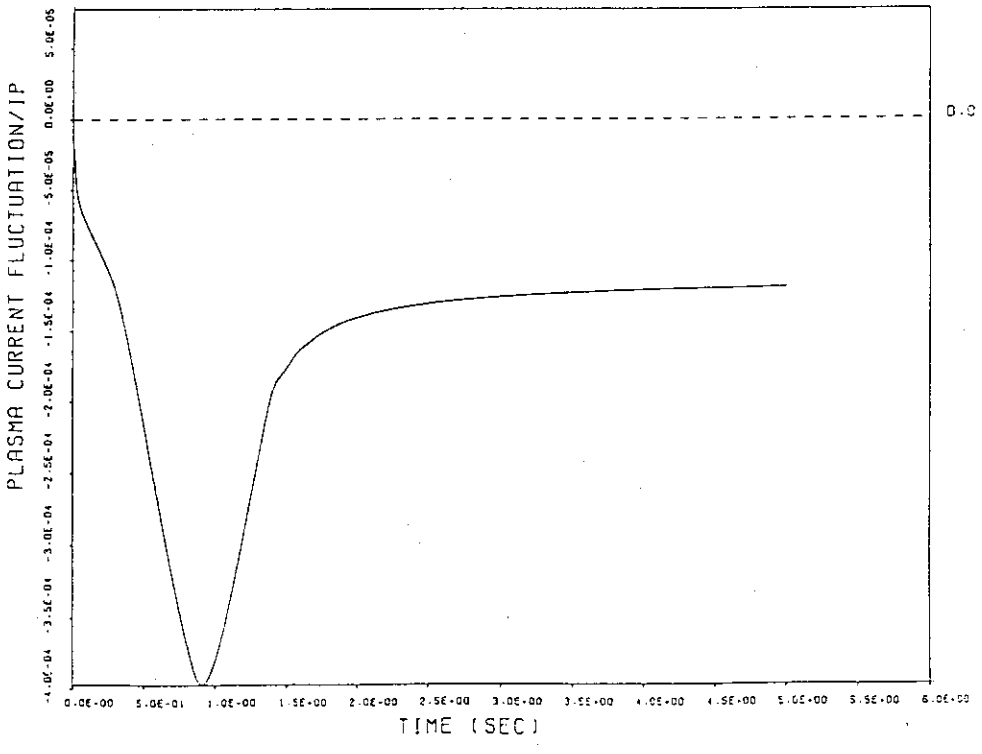

Fig. 5-2 Plasma current fluctuations

Fig. 5 The time evolution of the plasma position control (Outline Design)
(Plasma = Outline Design, Voltage limit = 3 V, $\delta B_r = 5$ G,
PF coils used = #2, 3, 5, 7)

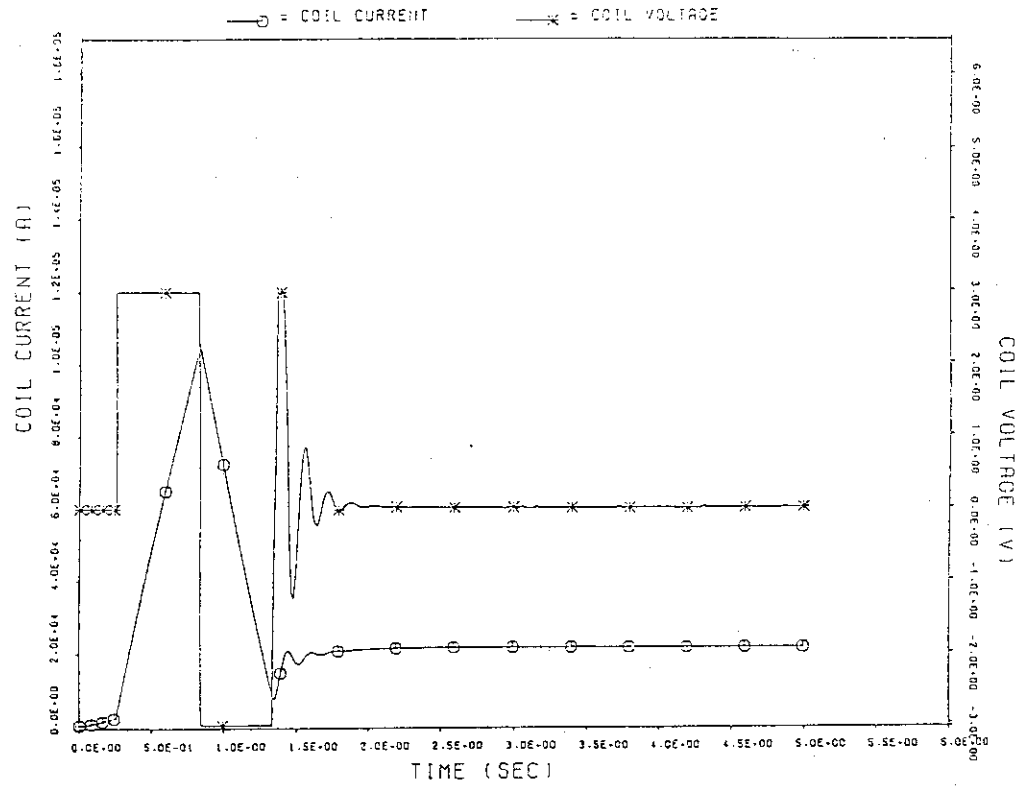

Fig. 5-3 The current and the voltage of PF2

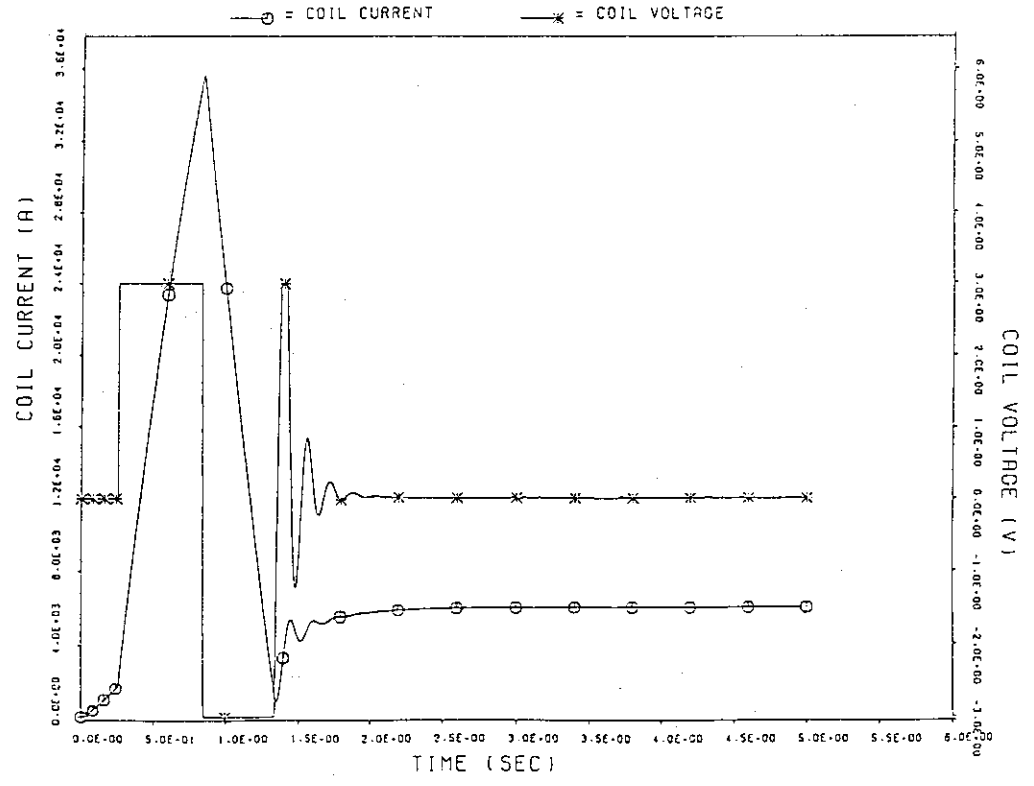

Fig. 5-4 The current and the voltage of PF3

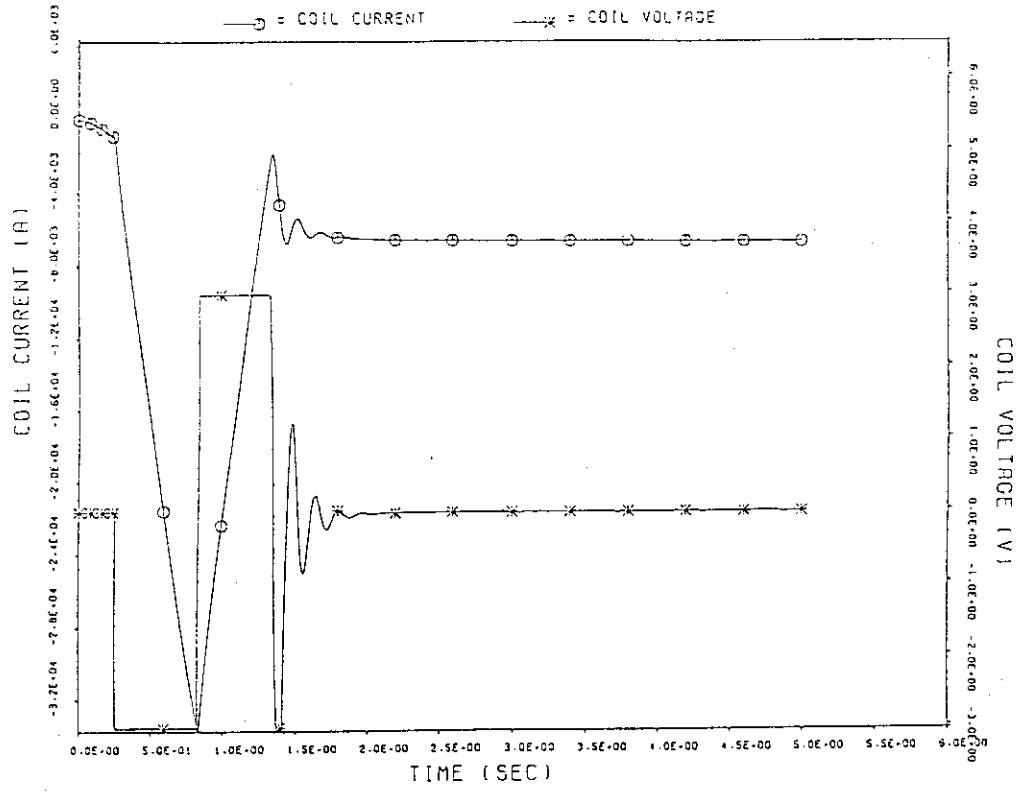

Fig. 5-5 The current and the voltage of PF5

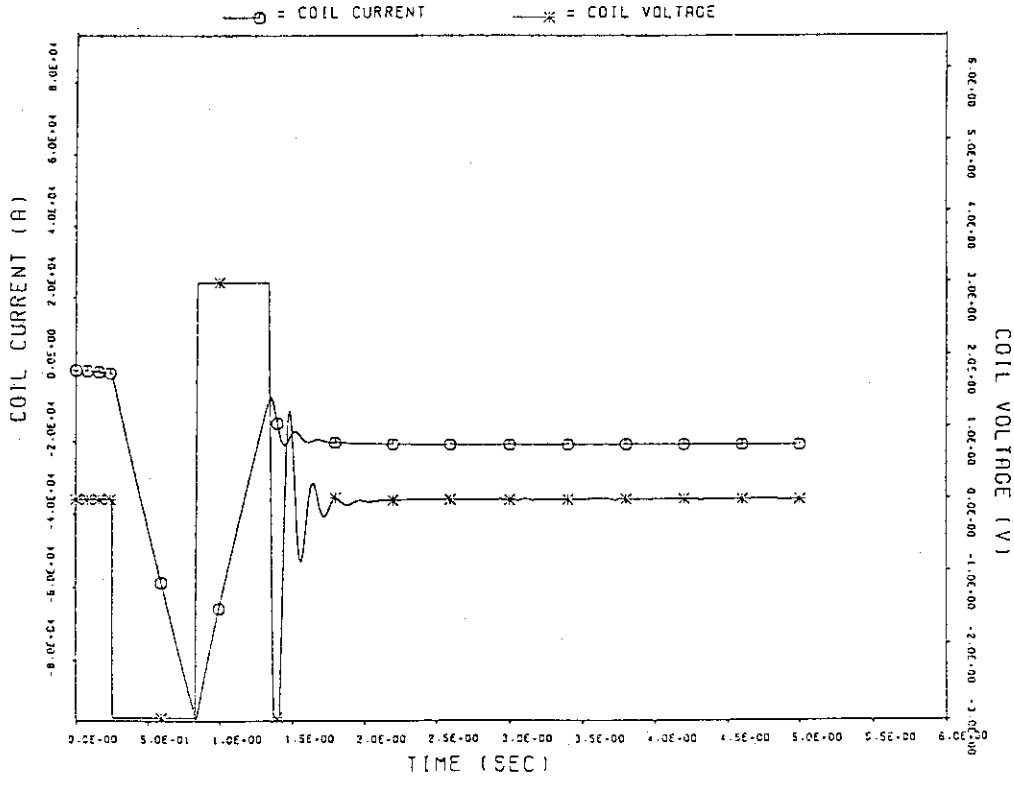

Fig. 5-6 The current and the voltage of PF7

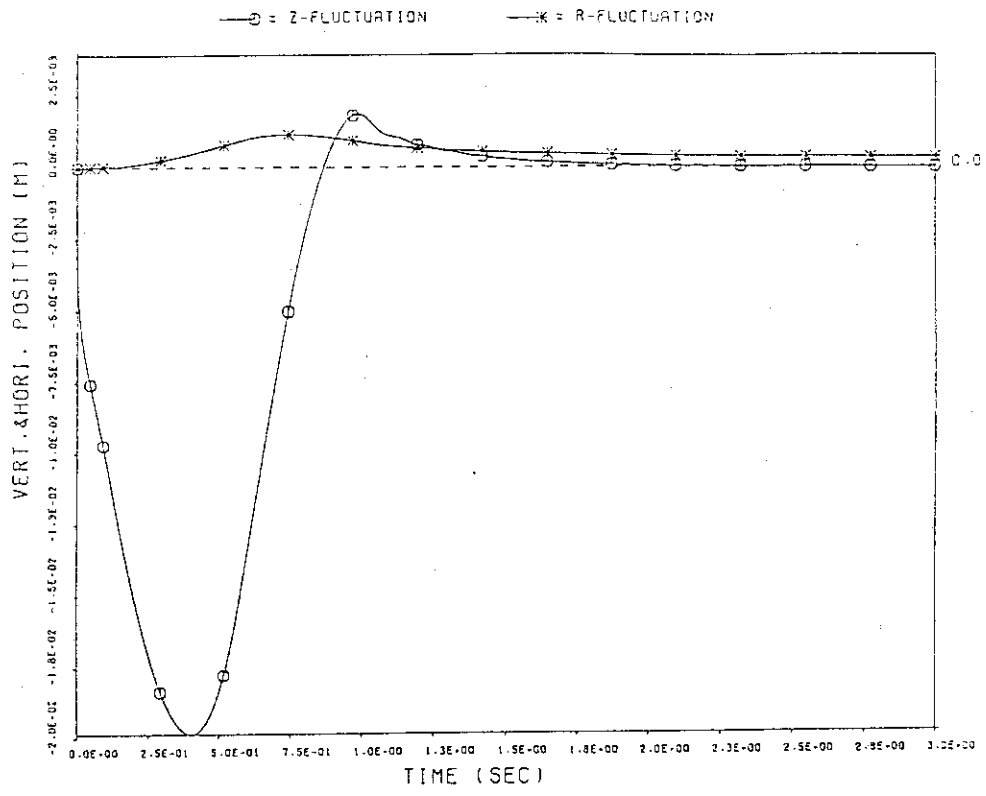

Fig. 6-1 Vertical and Horizontal plasma fluctuations

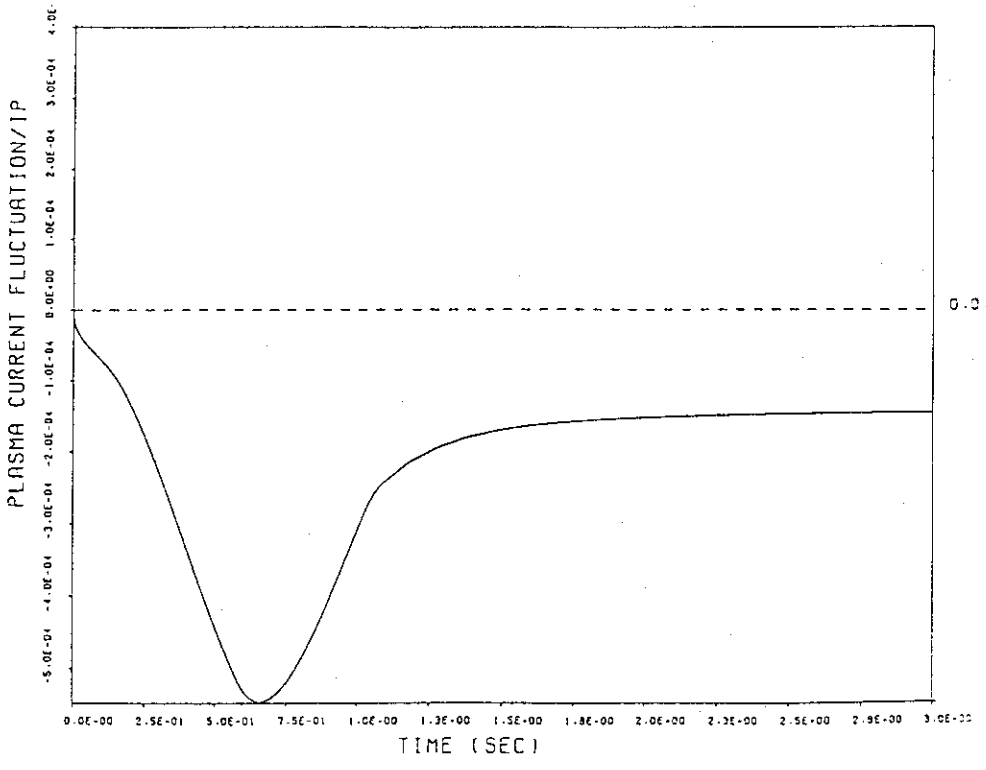

Fig. 6-2 Plasma current fluctuations

Fig. 6 The time evolution of the plasma position control (Case (E))
(Plasma = Case (E), Voltage limit = 5 V, $\delta B_r = 5$ G,
PF coils used = #2, 3, 5, 7)

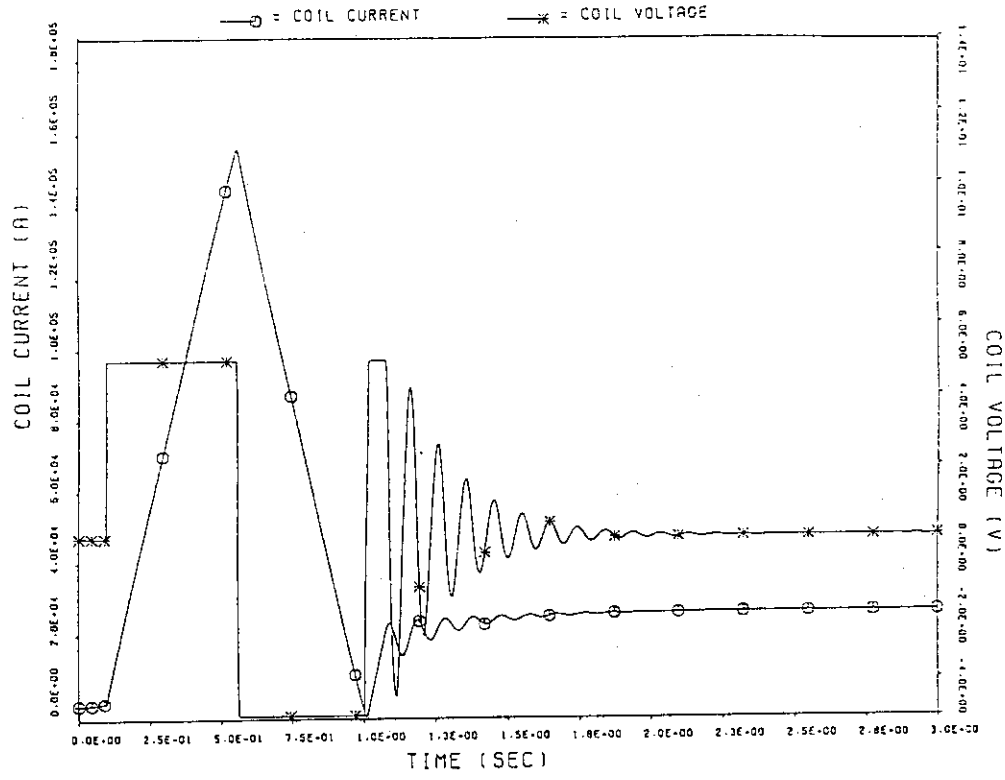

Fig. 6-3 The current and the voltage of PF2

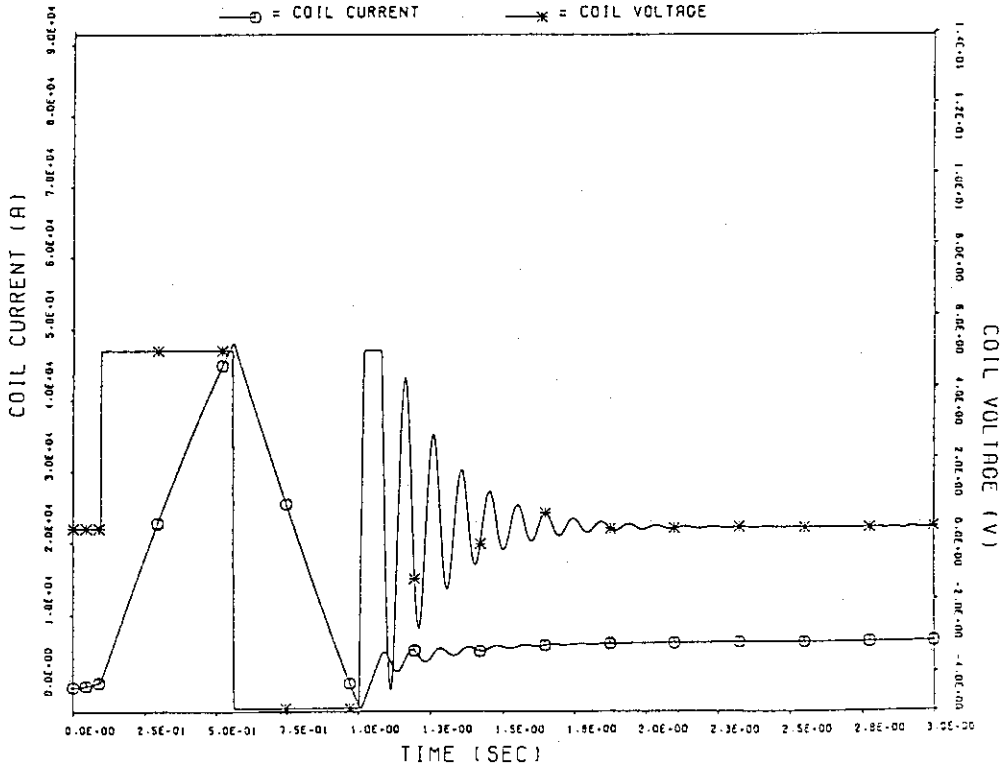

Fig. 6-4 The current and the voltage of PF3

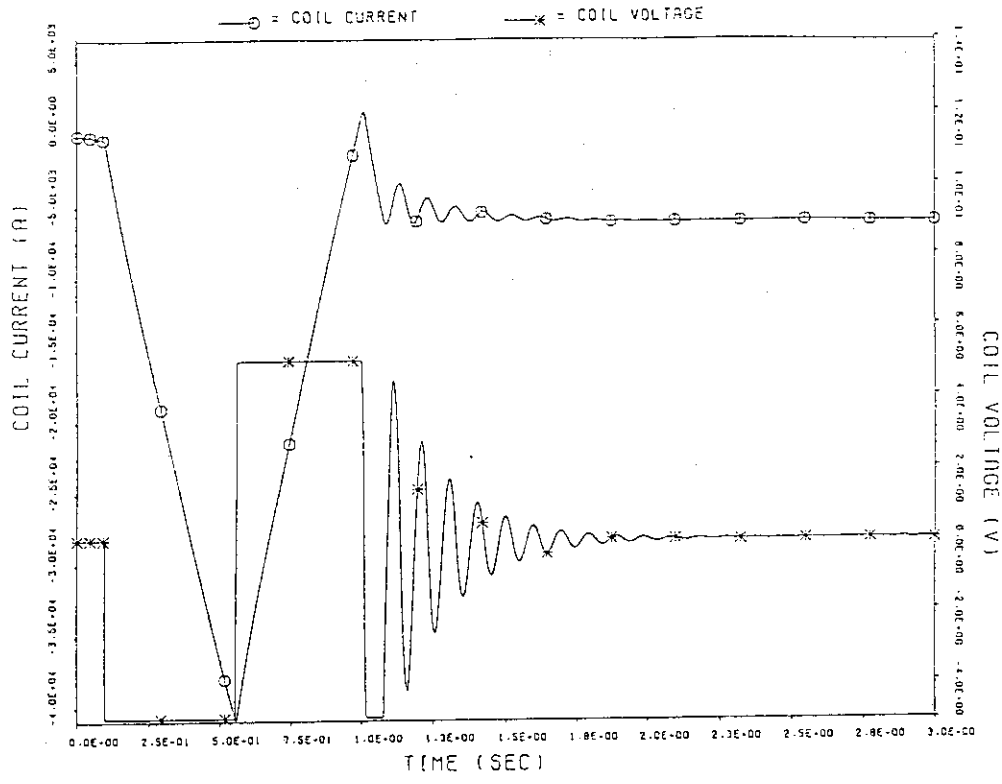

Fig. 6-5 The current and the voltage of PF5

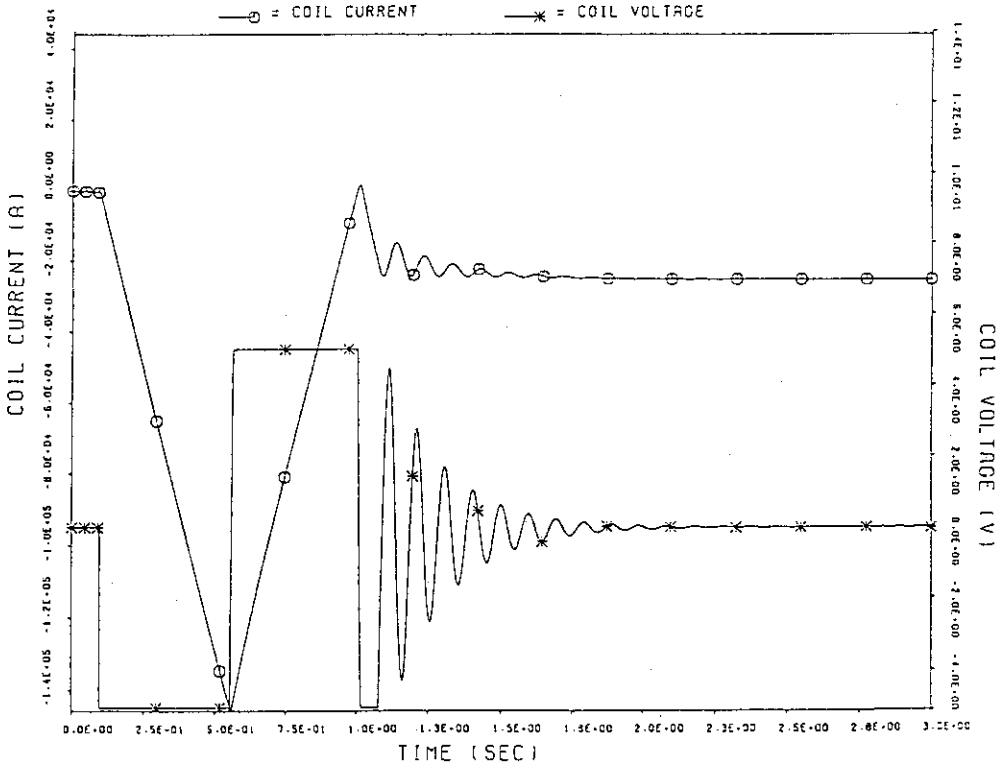

Fig. 6-6 The current and the voltage of PF7

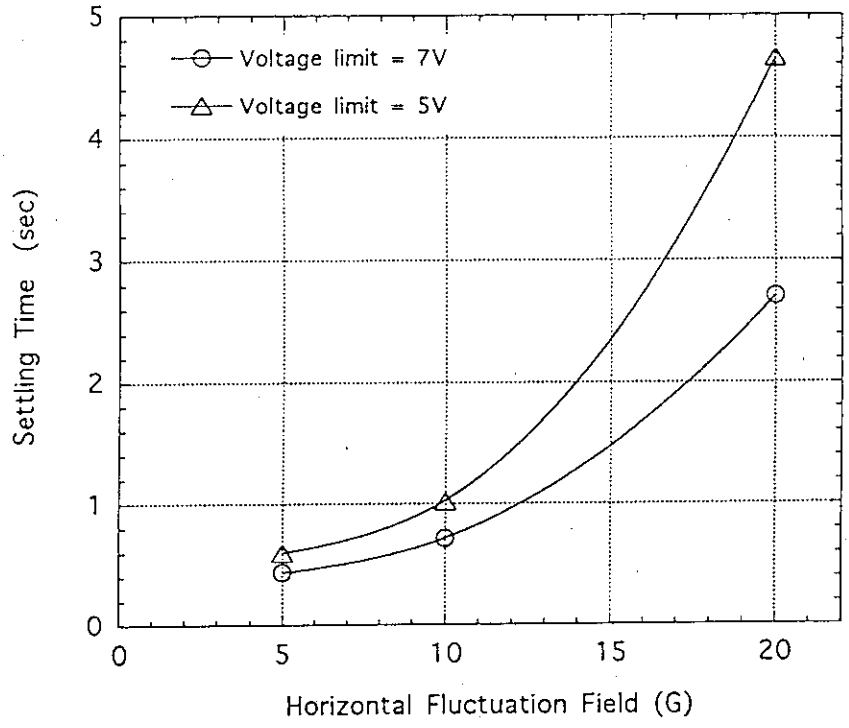

Fig. 7-1 Settling time vs. the control voltege limit

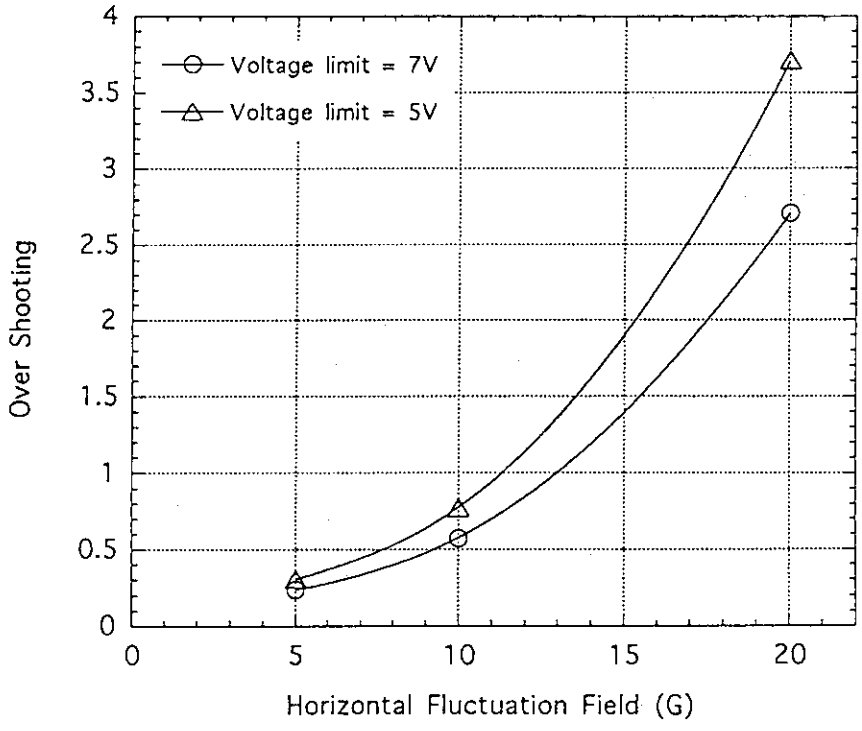

Fig. 7-2 Over shooting vs. the control voltage limit

Fig. 7 The dependence on the horizontal fluctuation field
(Plasma = Outline Design, PF coils #2, 3, 5, 7 are used)

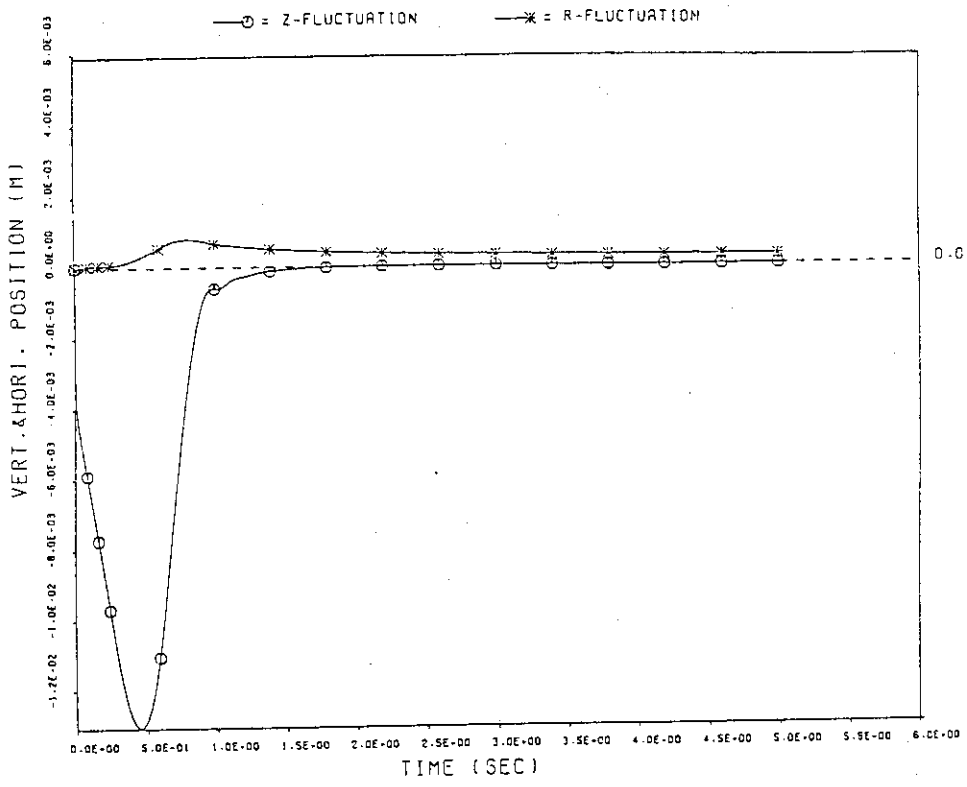

Fig. 8-1 Vertical and Horziontal motion for $\delta B_r = 5\,G$

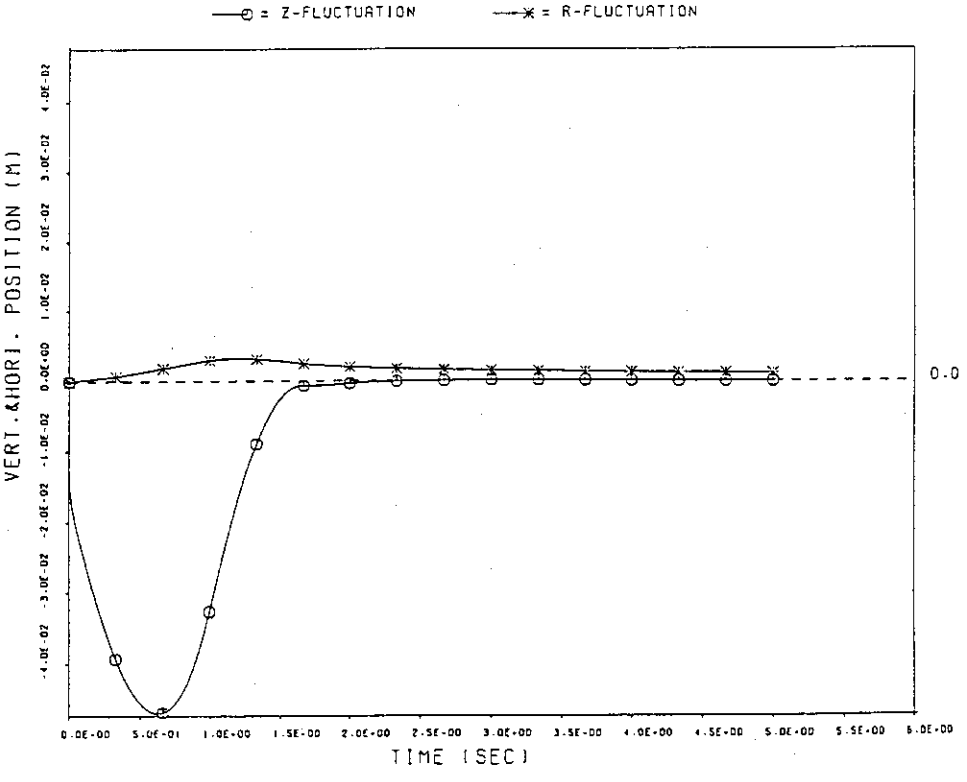

Fig. 8-2 Vertical and Horziontal motion for $\delta B_r = 20\,G$

Fig. 8 The position control for different horizontal fluctuation field (Plasma = Outline Design, Voltage limit = 5 V, PF #2, 3, 5, 7 are sued)

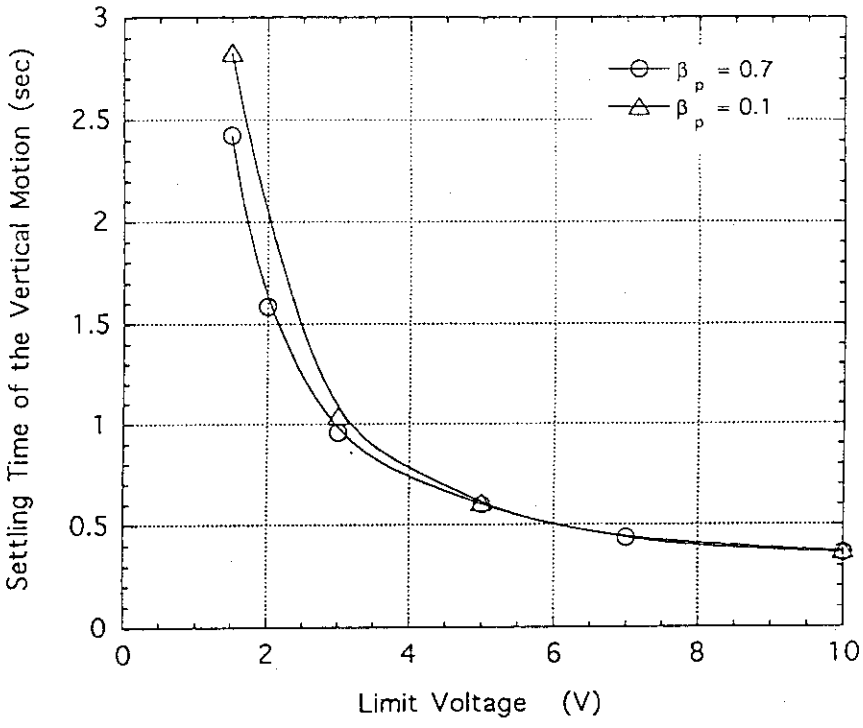

Fig. 9-1 Settling time vs. the voltage limit of the control coils

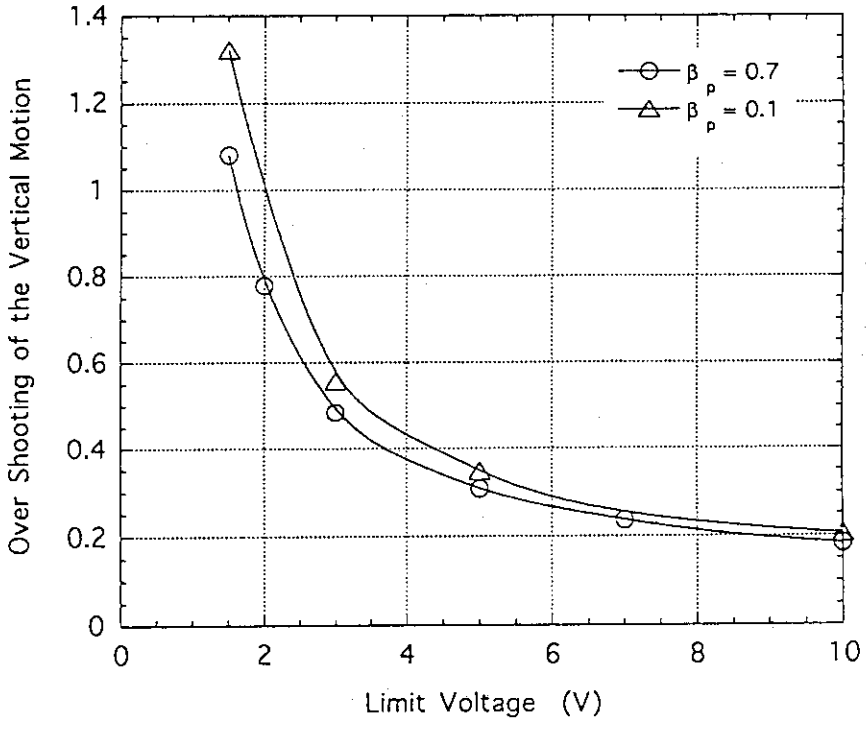

Fig. 9-2 Over shooting vs. the voltage limit of the control coils

Fig. 9 Simulation results of the Outline Design for different β_p
(Plasma = Outline Design, $\delta B_r = 5\,G$, $Z_0 = 1\,cm$)

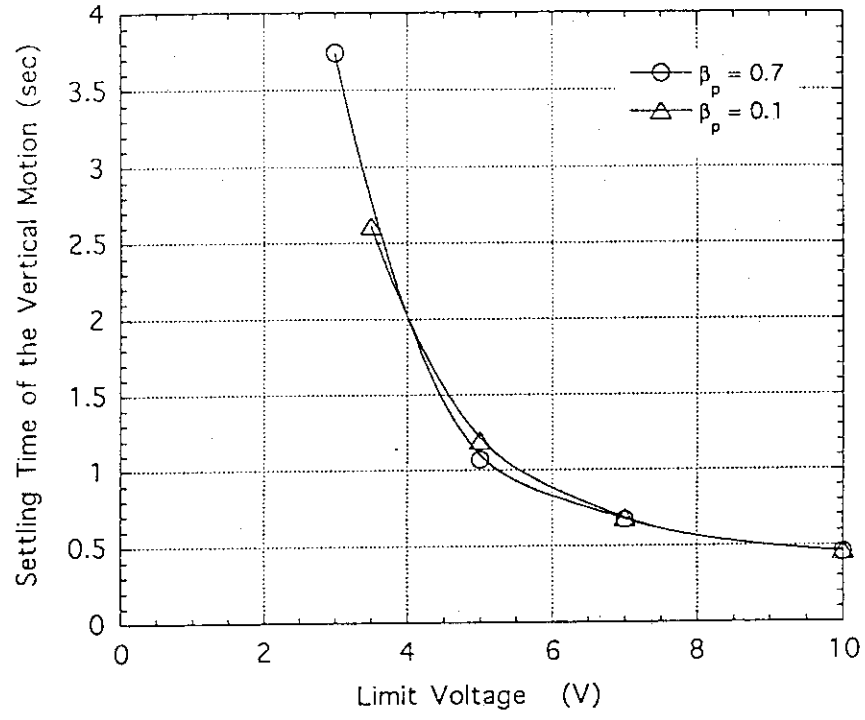

Fig. 10-1 Settling time vs. the voltage limit of the control coils

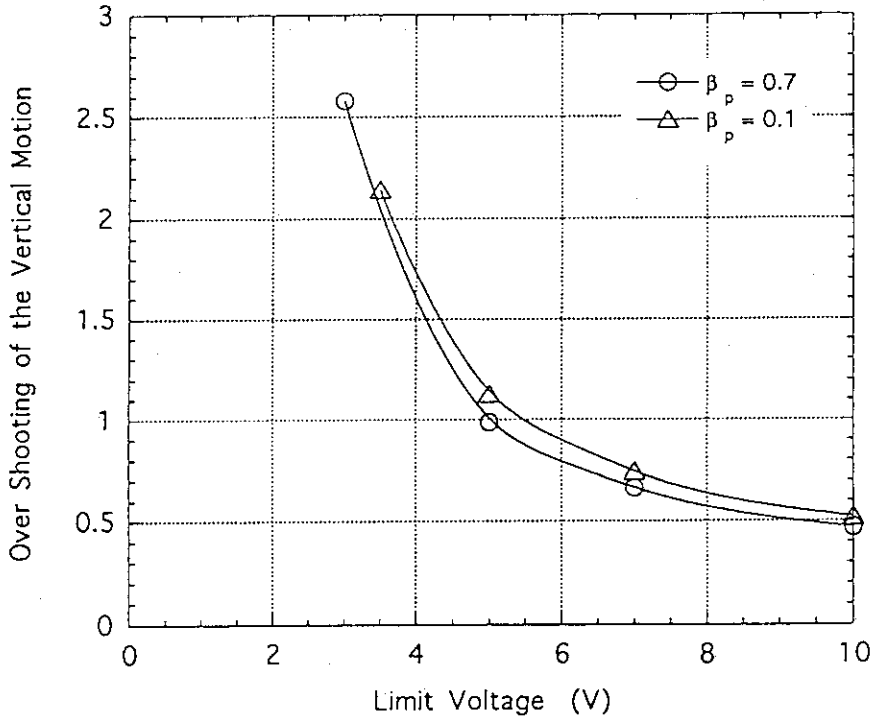

Fig. 10-2 Over shooting vs. the voltage limit of the control coils

Fig. 10 Simulation results of the Case (E) for different β_p
(Plasma = Case (E), $\delta B_r = 5\,G$, $Z_0 = 1\,cm$)

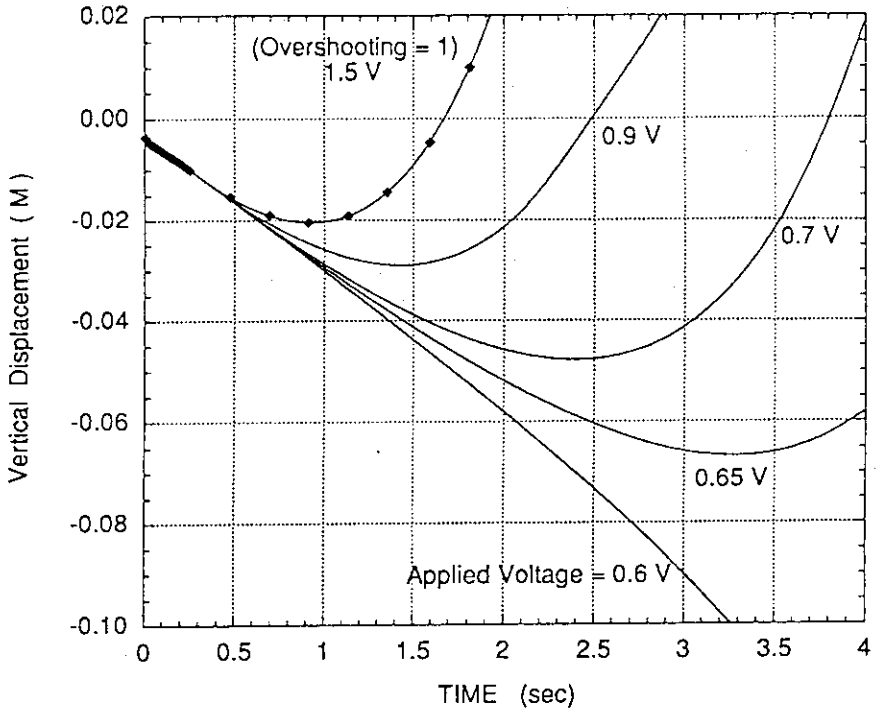

Fig. 11-1 Start control when the plasma moves 1 cm ($Z_0 = 1$ cm)

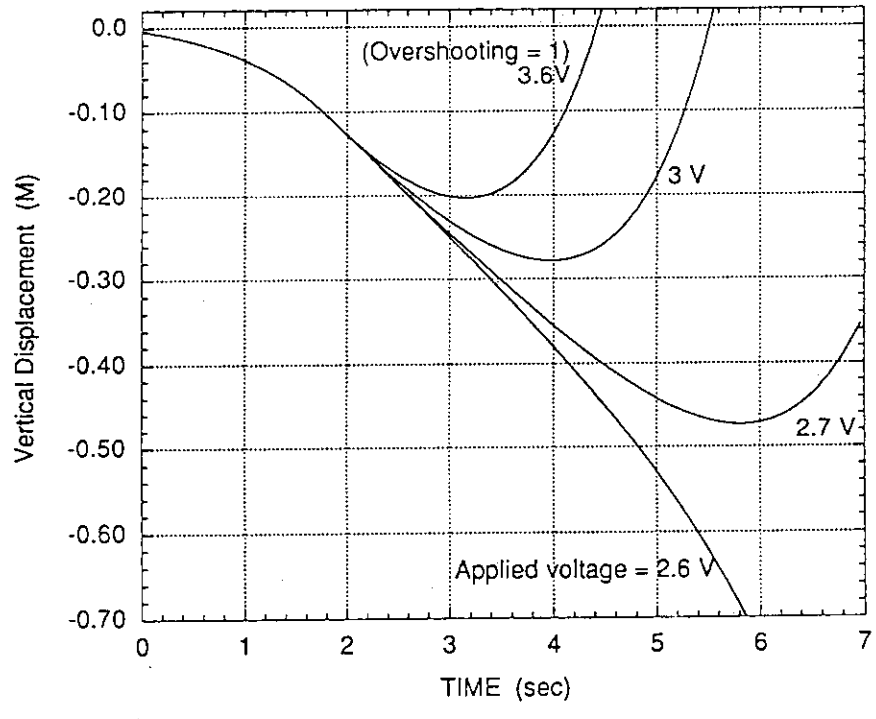

Fig. 11-2 Start control when the plasma moves 10 cm ($Z_0 = 10$ cm)

Fig. 11 Z_0-dependence in the simulations applying constant voltage
(Outline Design (100 $\mu\Omega$ FW) PF coil #2 - #7 used, $\delta B_r = 5$ G)

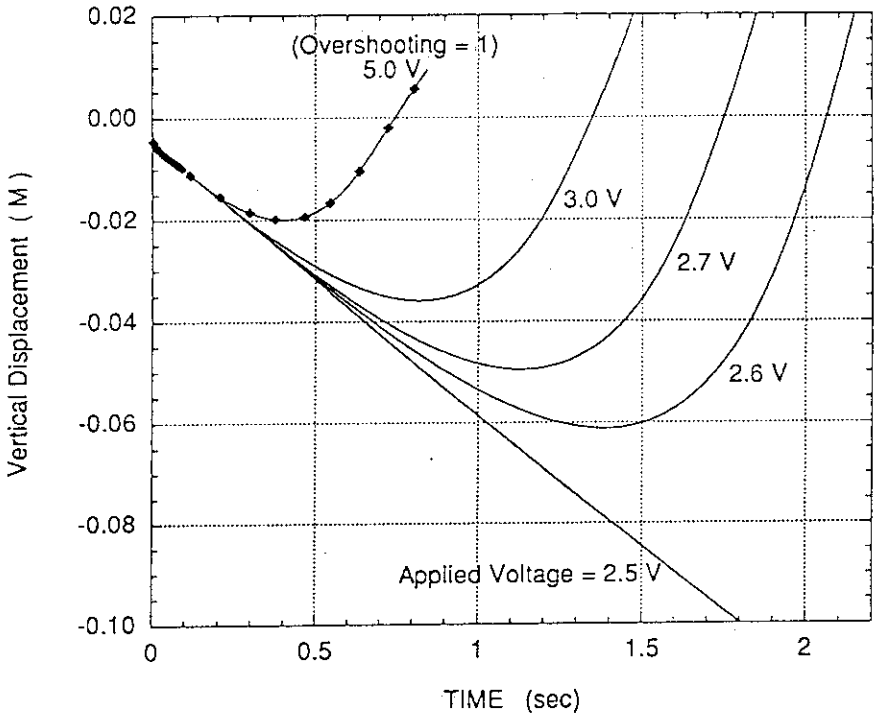

Fig. 12-1 Start control when the plasma moves 1 cm ($Z_0 = 1$ cm)

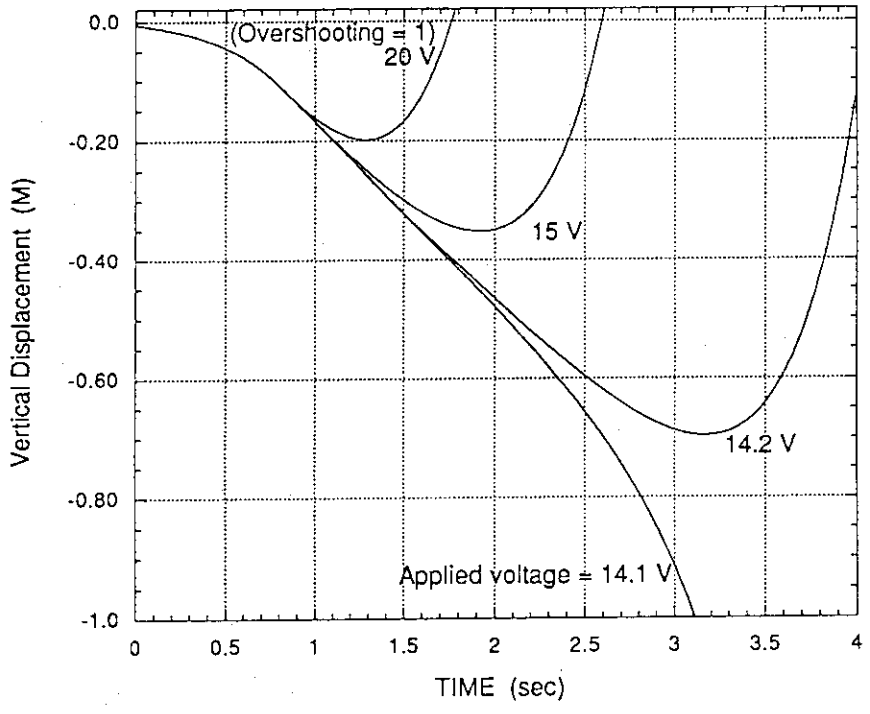

Fig. 12-2 Start control when the plasma moves 10 cm ($Z_0 = 10$ cm)

Fig. 12 Z_0-dependence in the simulations applying constant voltage (CASE (E) (100 $\mu\Omega$ FW) PF coil #2 - #7 used, $\delta B_r = 5$ G)

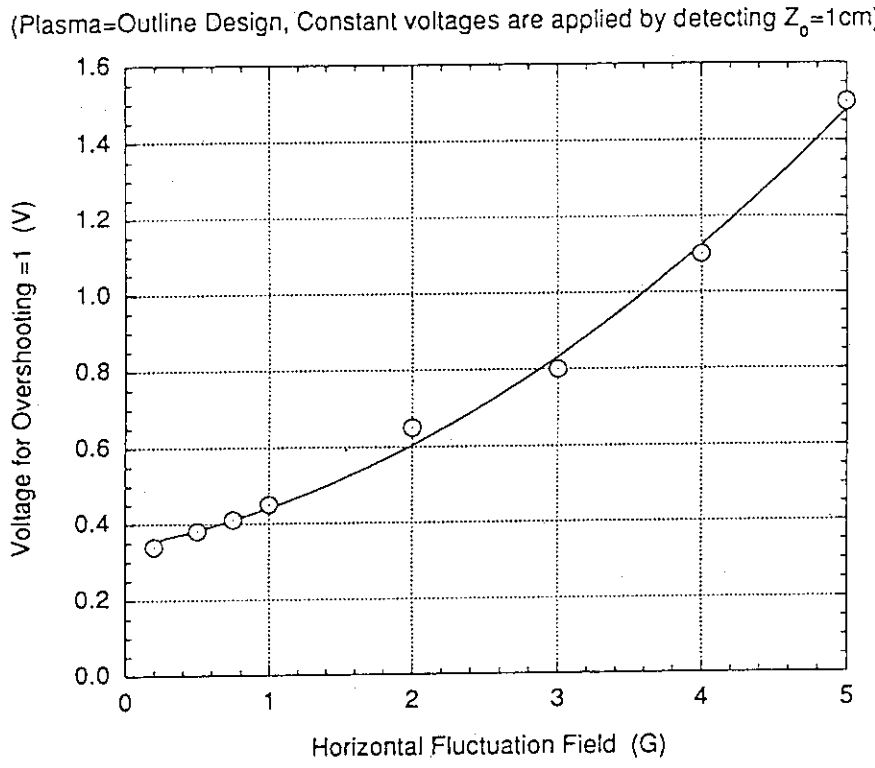

Fig. 13-1 The horizontal fluctuation field vs. applied voltages when overshooting = 1 for the Outline Design

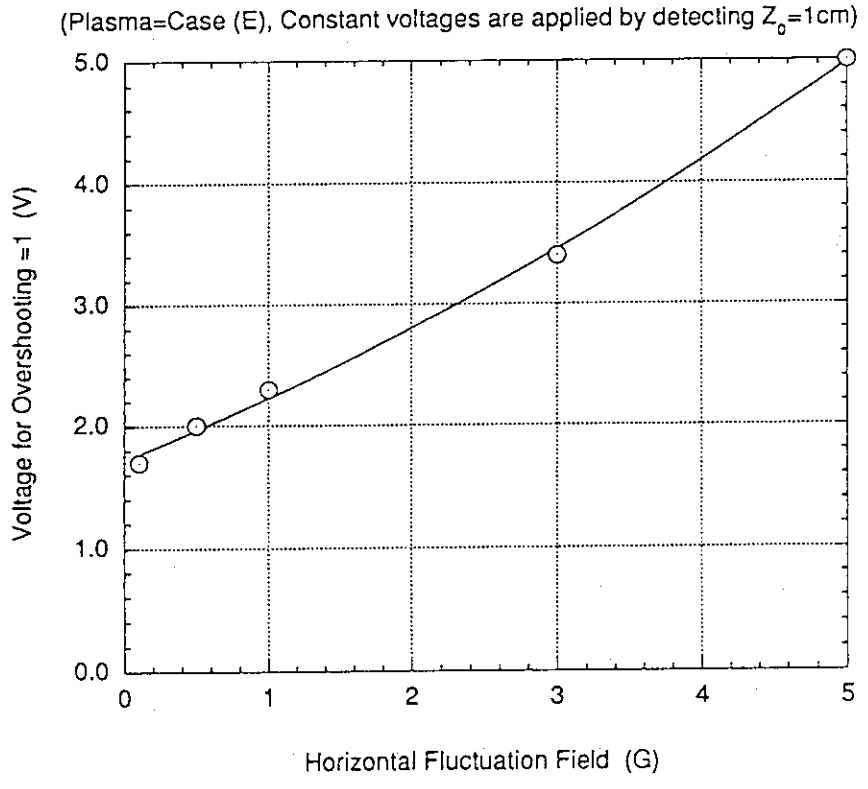

Fig. 13-2 The horizontal fluctuation field vs. applied voltages when overshooting = 1 for Case (E)

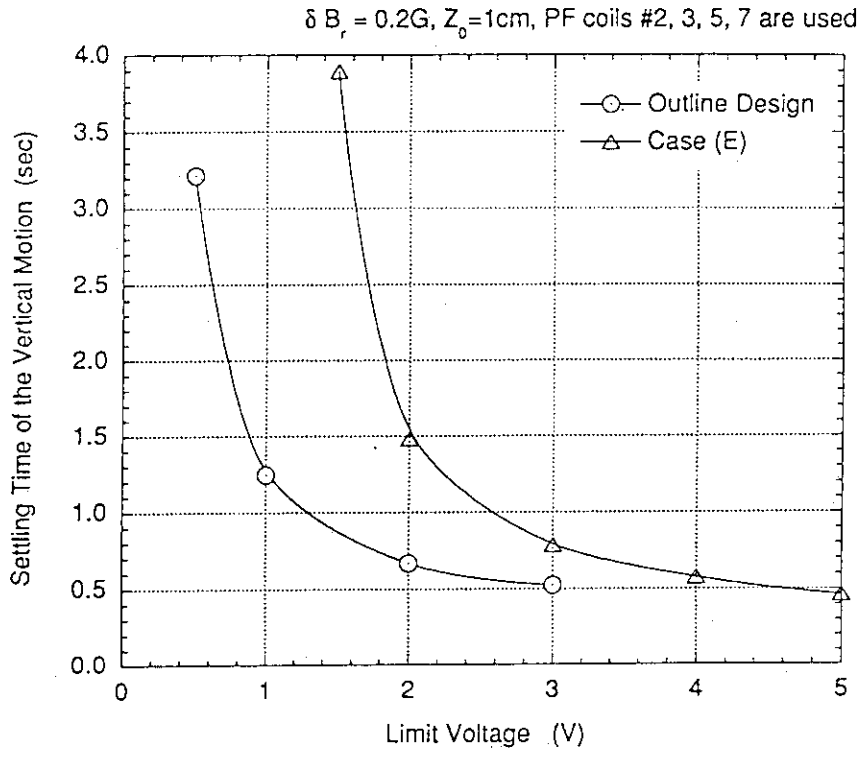

Fig. 14-1 The settling time and limit voltage for the control of $\delta B_r = 0.2\,G$

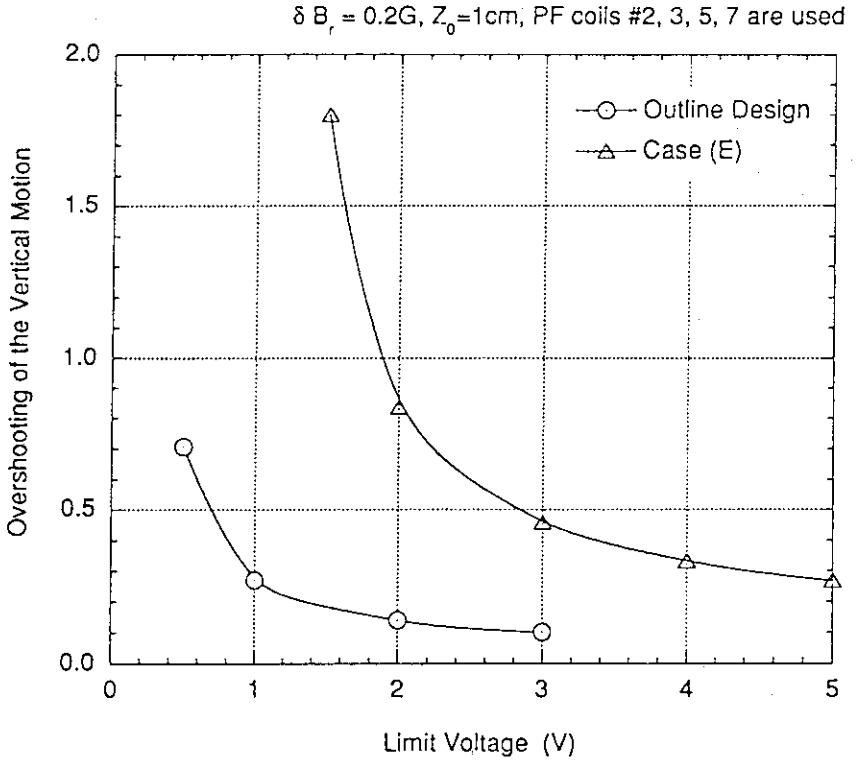

Fig. 14-2 The overshooting and limit voltage for the control of $\delta B_r = 0.2\,G$

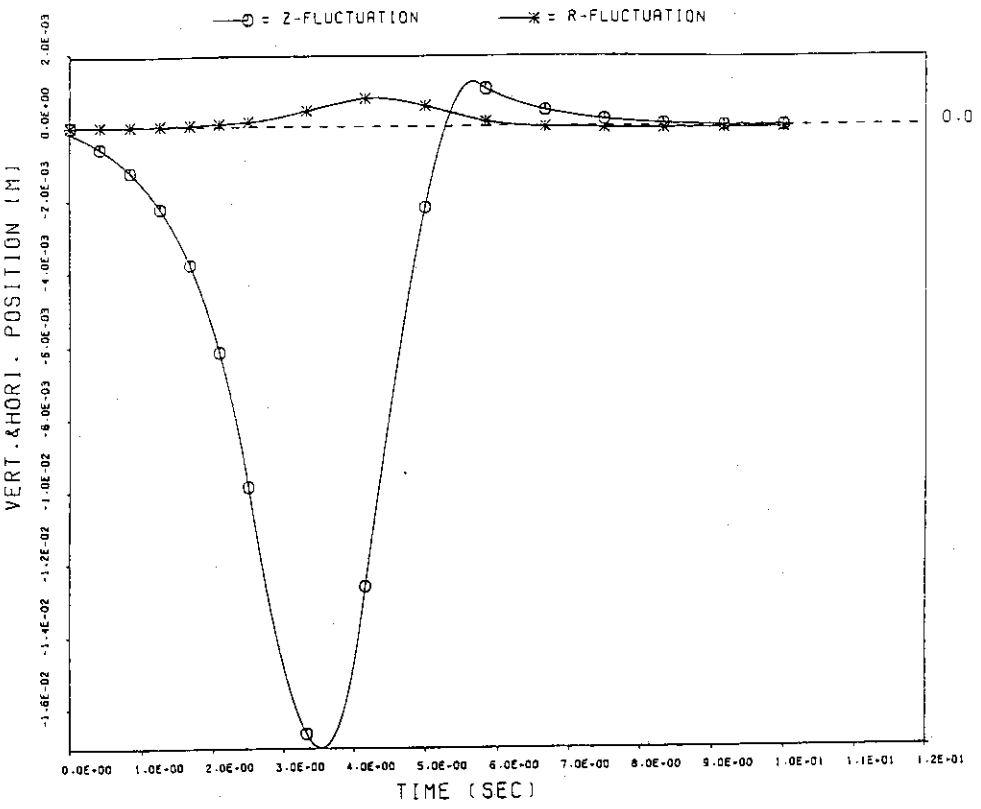

Fig. 15-1 Vertical and Horizontal Plasma fluctuations

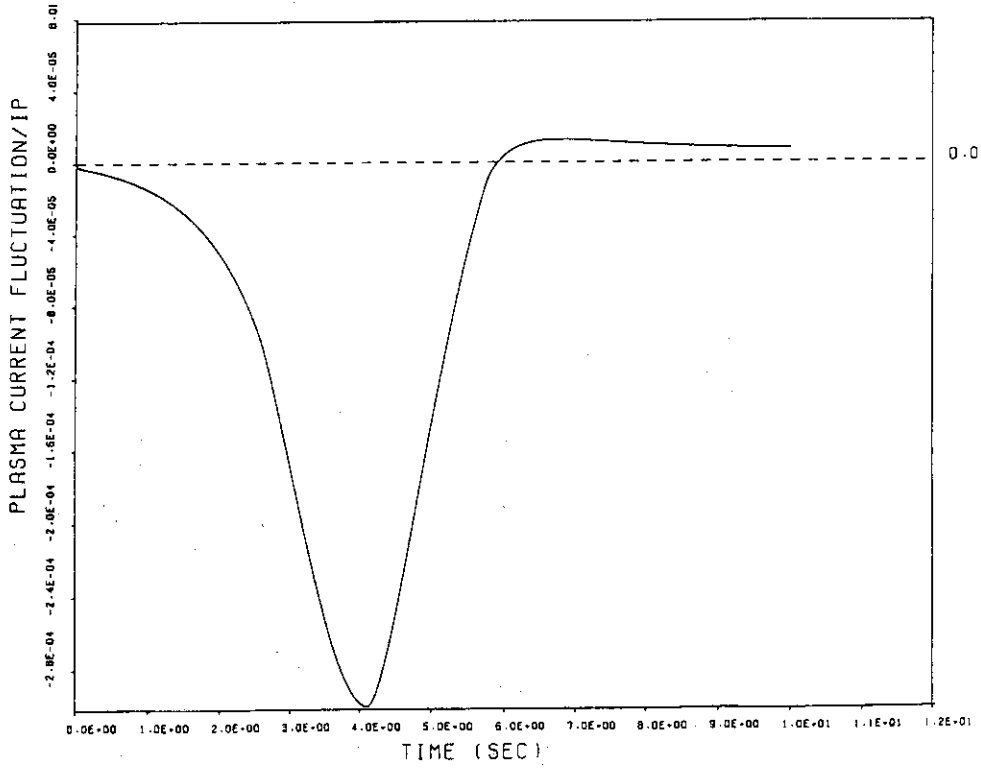

Fig. 15-2 Plasma current fluctuations

Fig. 15 The time evolution of the plasma position control (Outline Design, $\delta B_r = 0.2$ G)
(Plasma = Outline Design, $\delta B_r = 0.2$ G, $Z_0 = 1$ cm, Limit voltage = 0.5 V, PF #2, 3, 5, 7 are used)

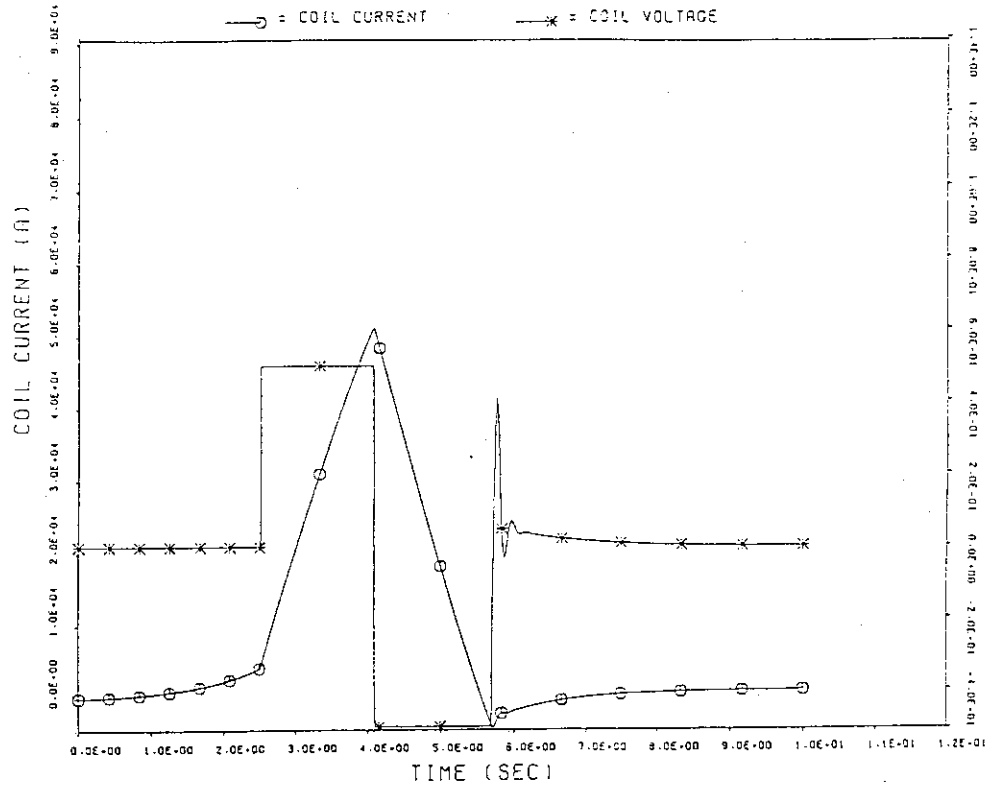

Fig. 15-3 The current and the voltage of PF2

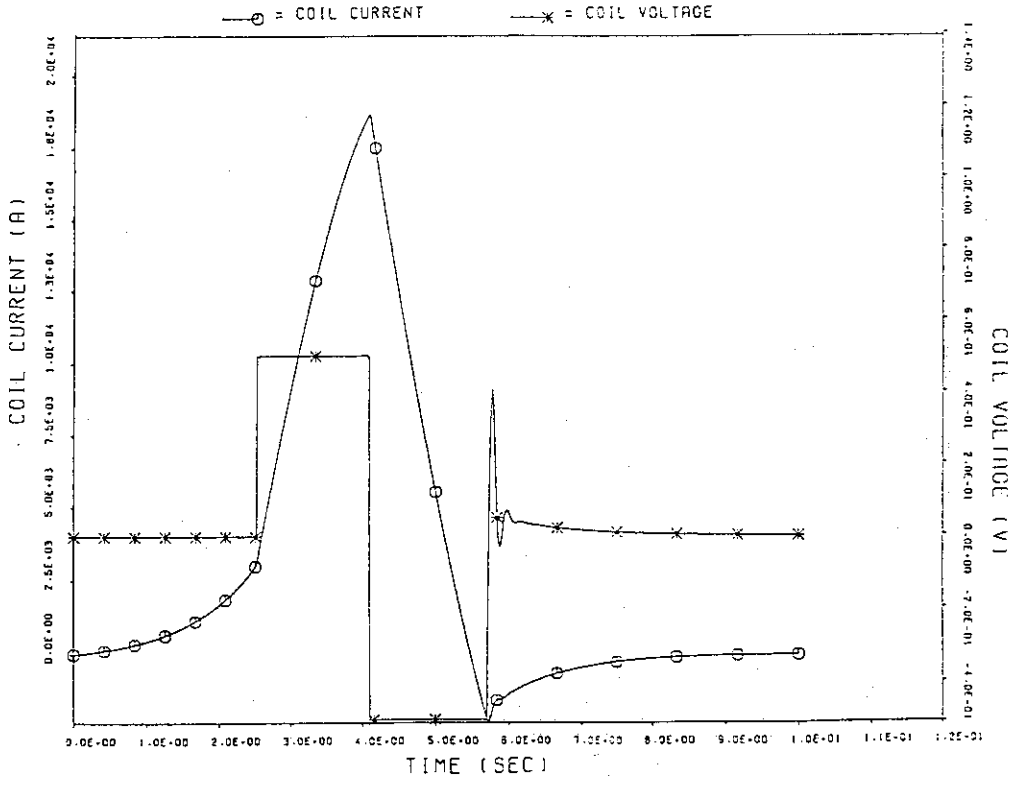

Fig. 15-4 The current and the voltage of PF3

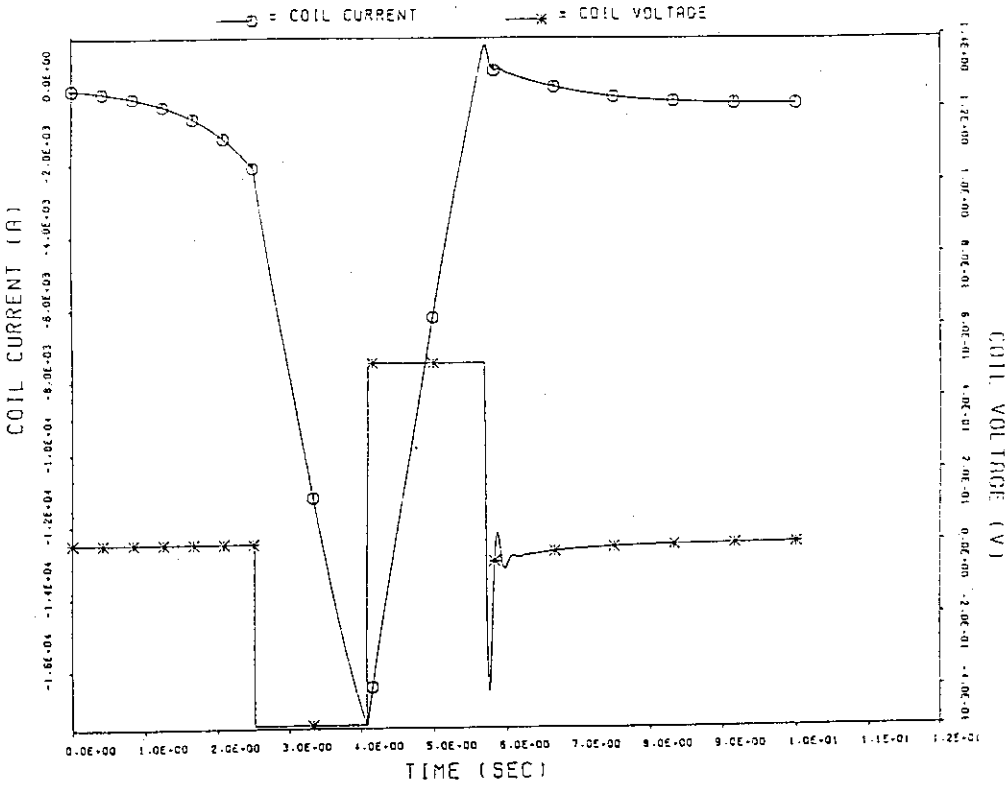

Fig. 15-5 The current and the voltage of PF5

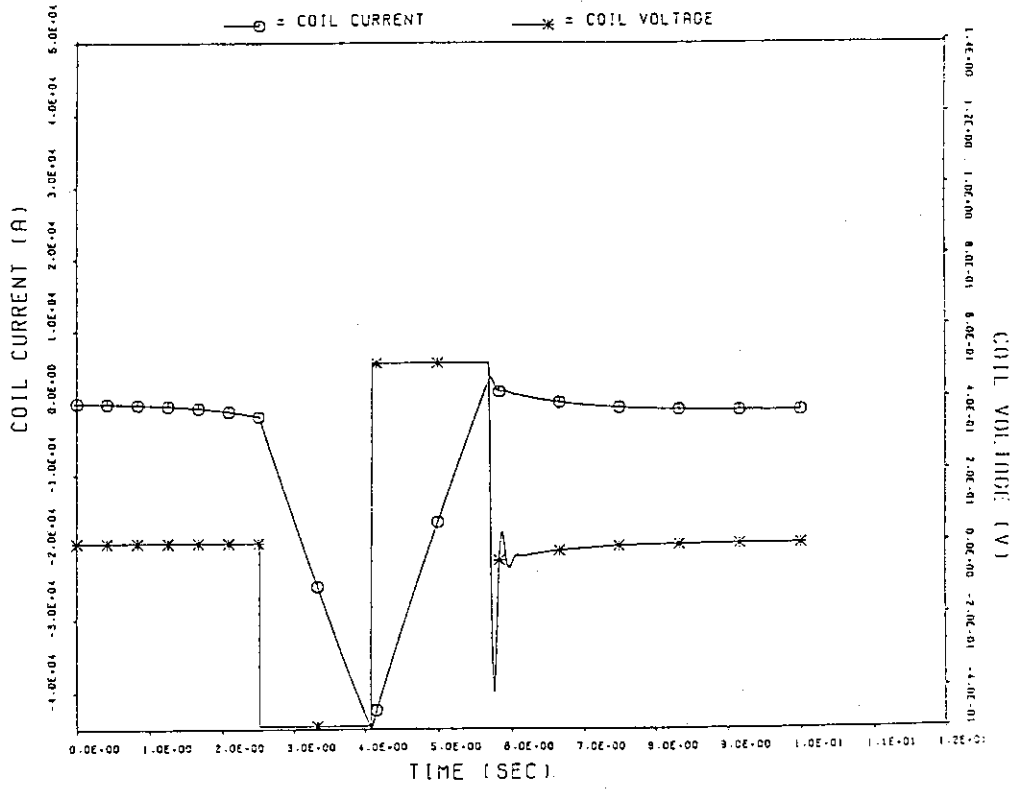

Fig. 15-6 The current and the voltage of PF7

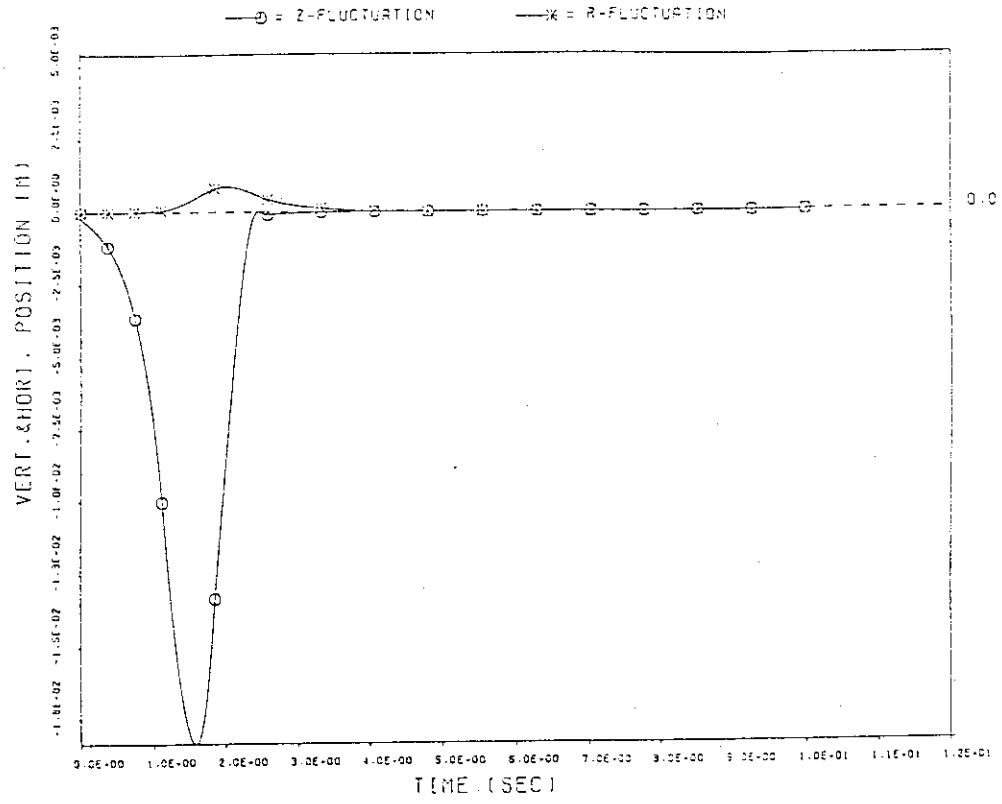

Fig. 16-1 Vertical and Horizontal plasma fluctuations

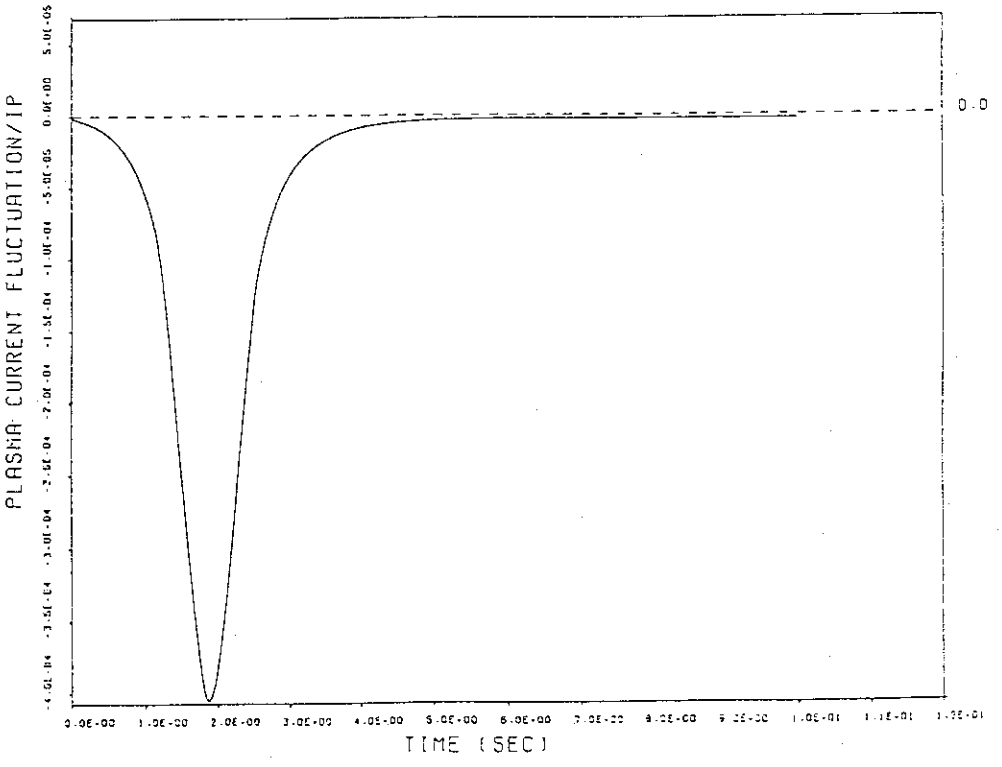

Fig. 16-2 Plasma current fluctuations

Fig. 16 The time evolution of the plasma position control (Case (E), $\delta B_r = 0.2$ G) (Plasma = Case (E), $\delta B_r = 0.2$ G, $Z_0 = 1$ cm, Limit voltage = 2 V, PF #2, 3, 5, 7 are used)

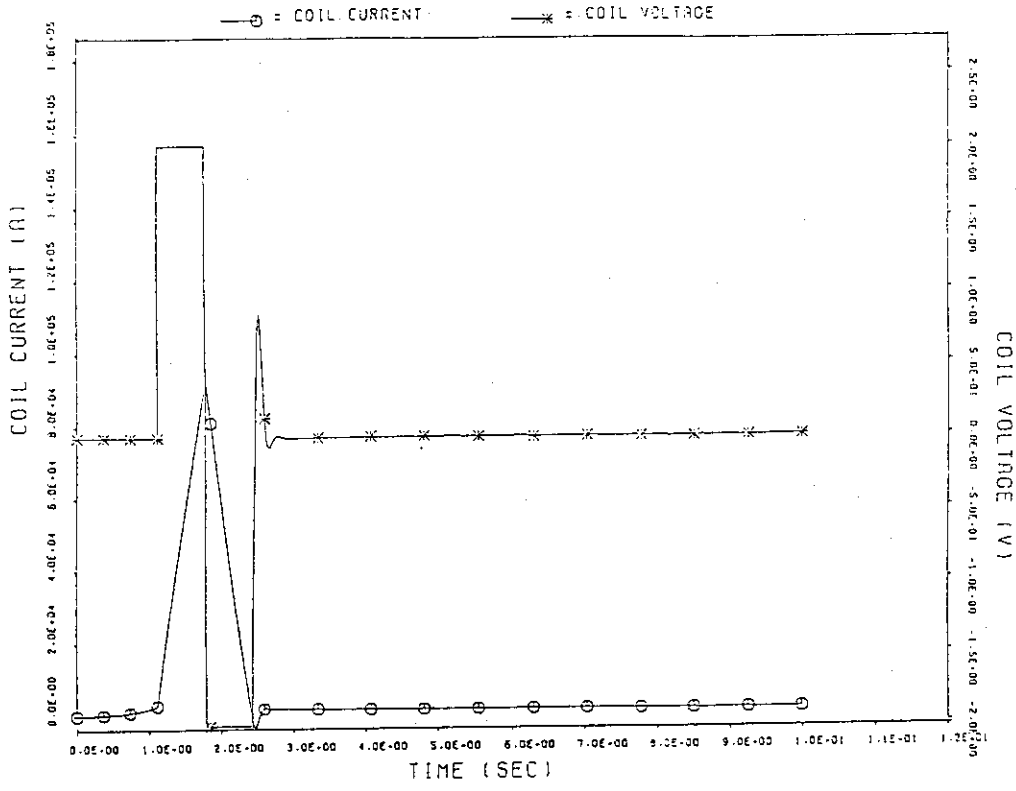

Fig. 16-3 The current and the voltage of PF2

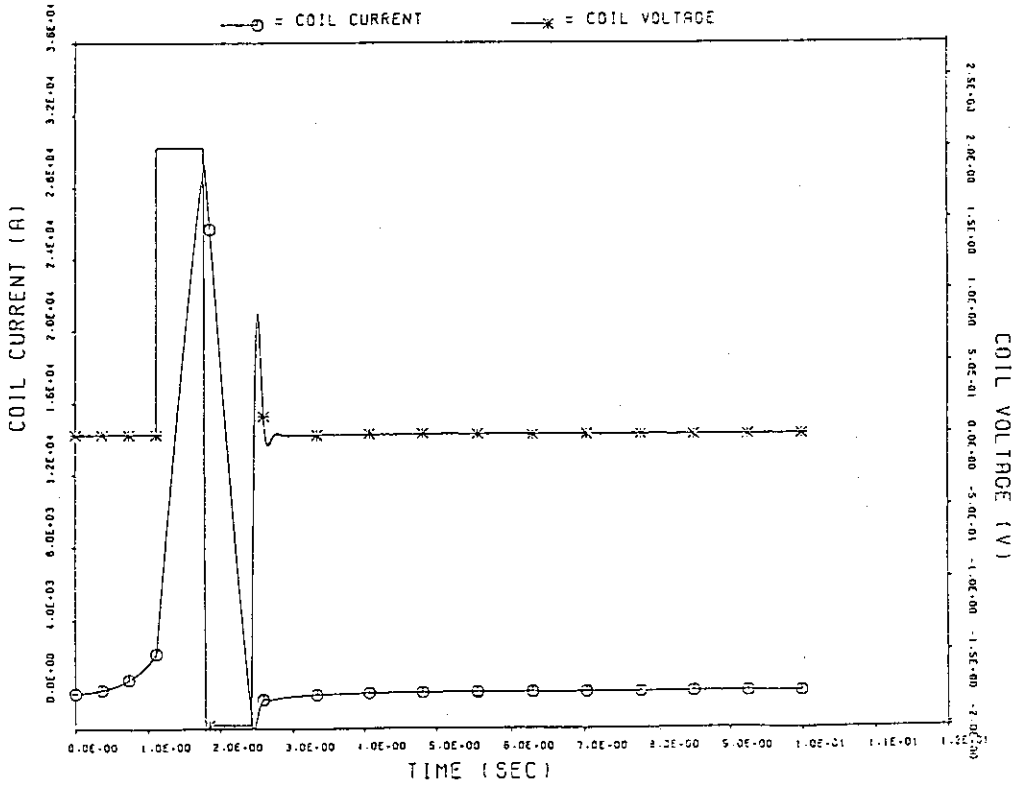

Fig. 16-4 The current and the voltage of PF3

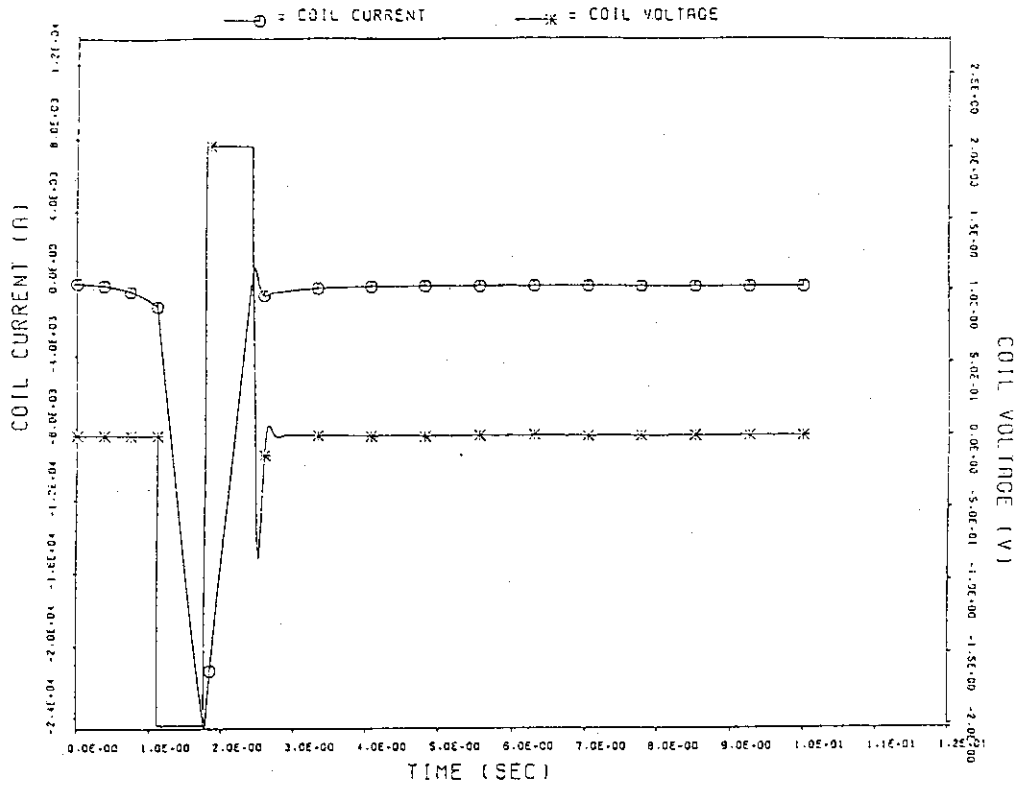

Fig. 16-5 The current and the voltage of PF5

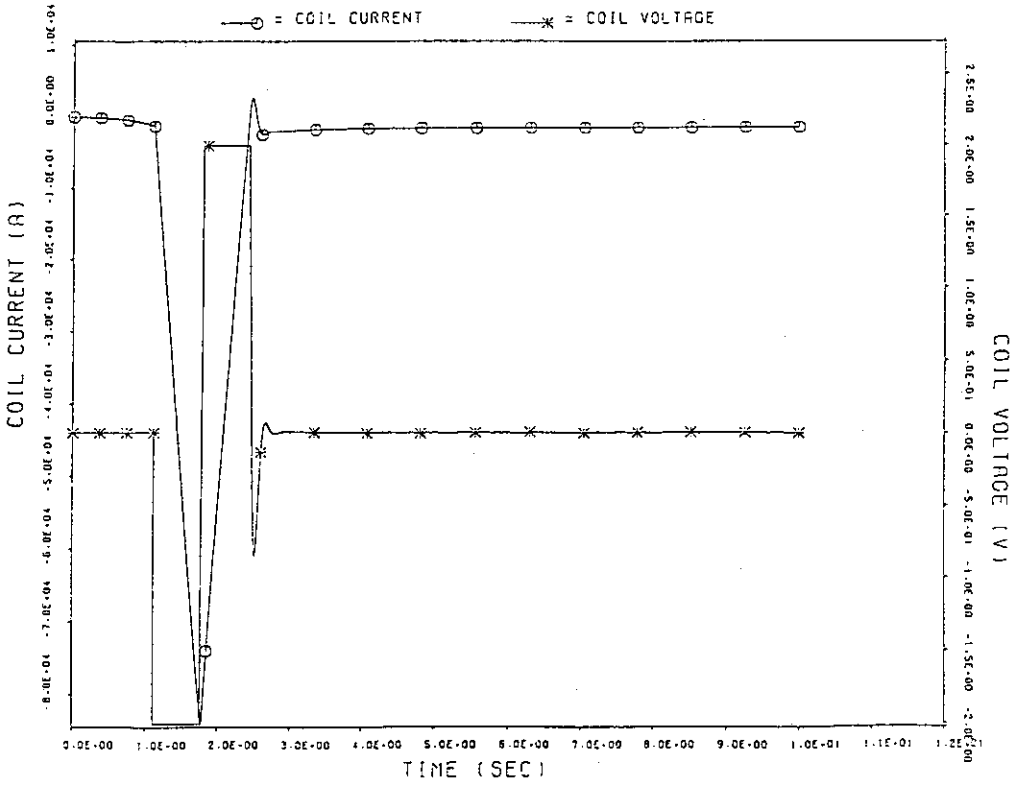

Fig. 16-6 The current and the voltage of PF7

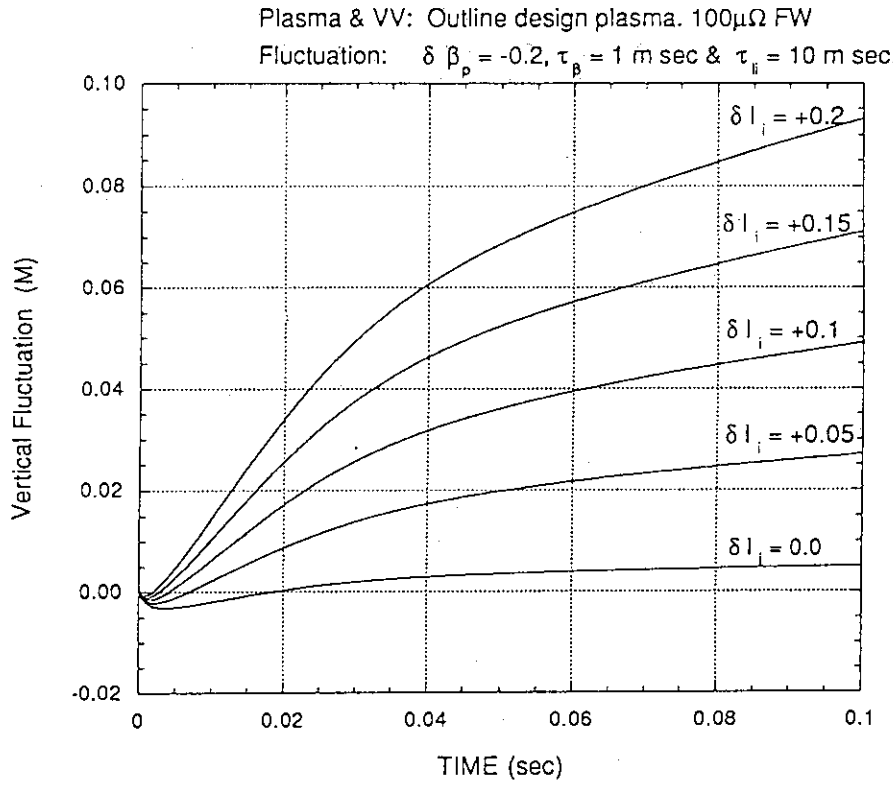

Fig. 17-1 The vertical motion for the increse of the internal inductance

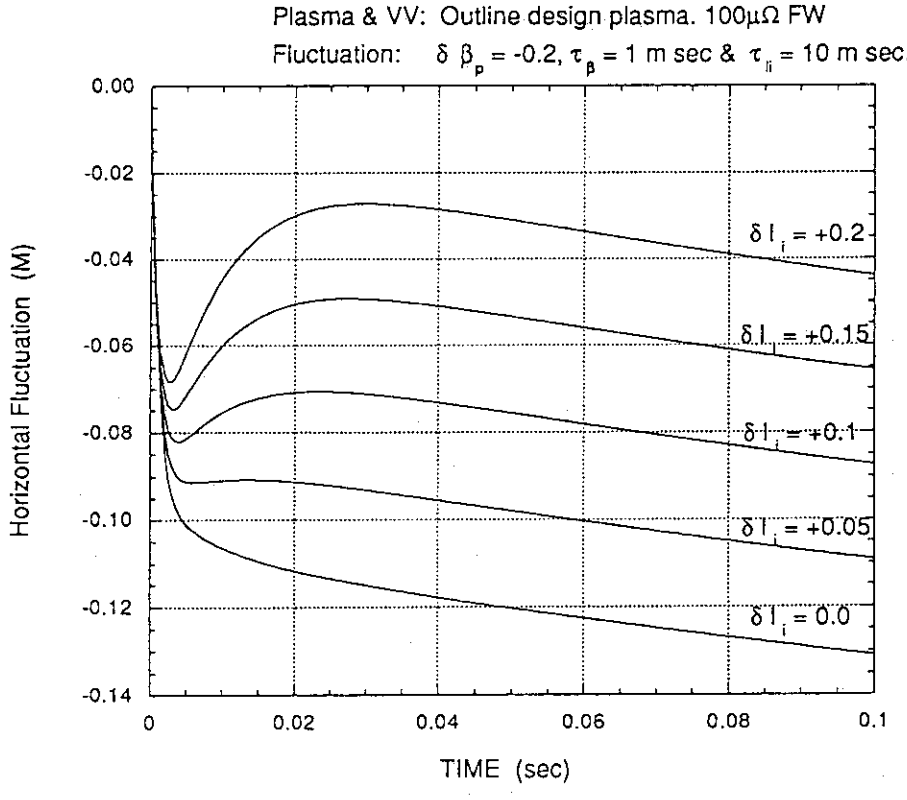

Fig. 17-2 The horizontal motion for the increse of the internal inductance

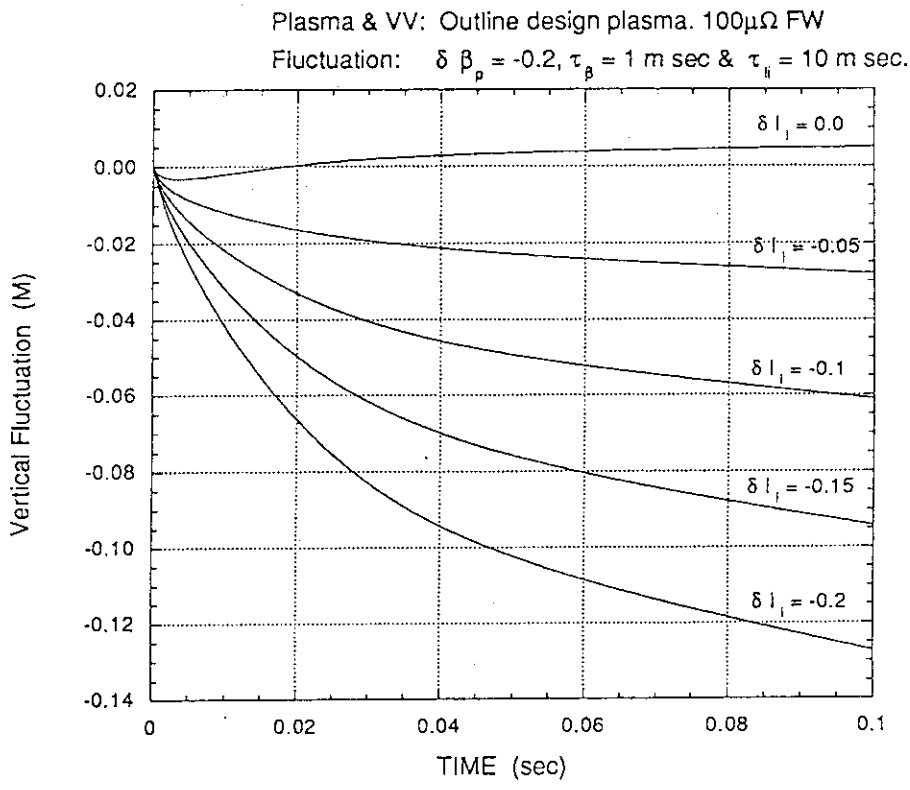

Fig. 18-1 The vertical motion for the drop of the internal inductance

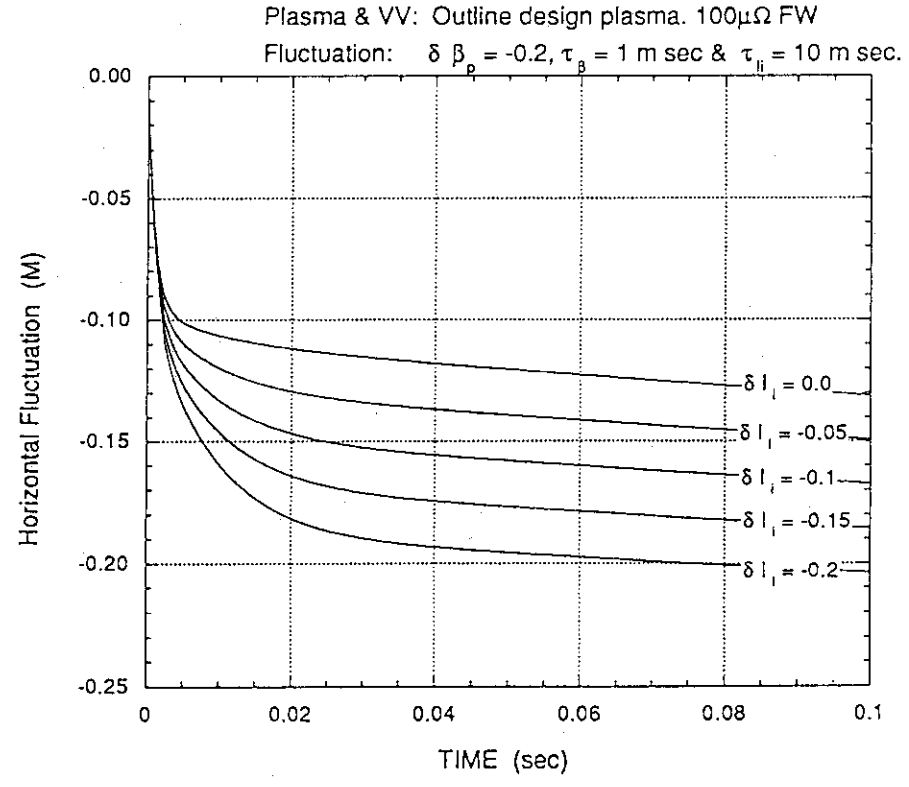

Fig. 18-2 The horizontal motion for the drop of the internal inductance

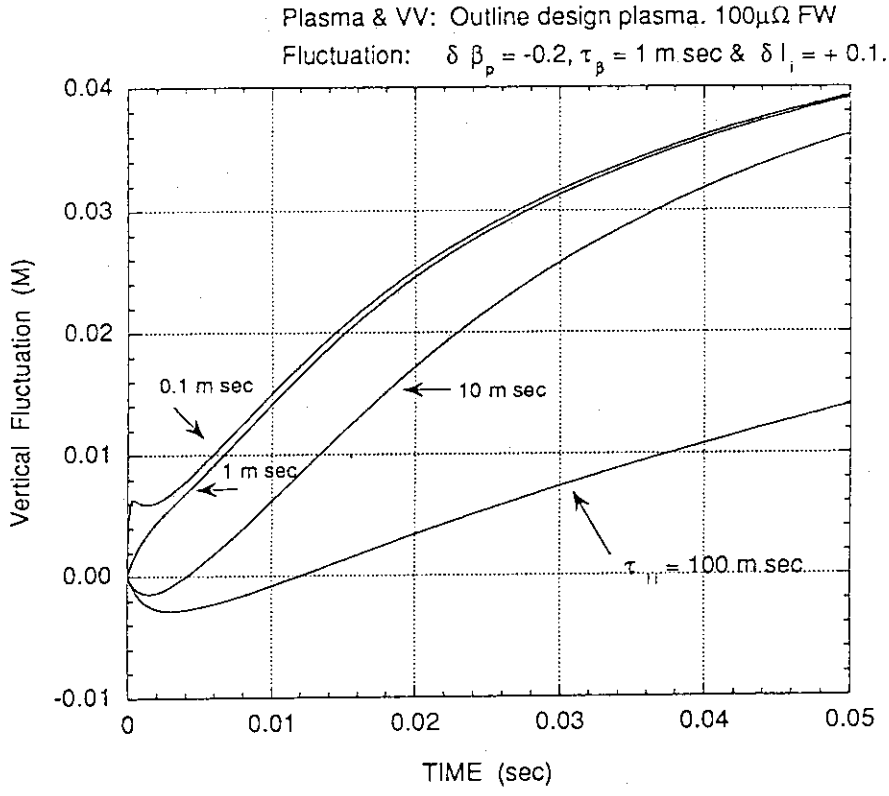

Fig. 19-1 The time constant of $\delta \ell_i$ vs. the vertical motion for $\delta \ell_i$ increase.

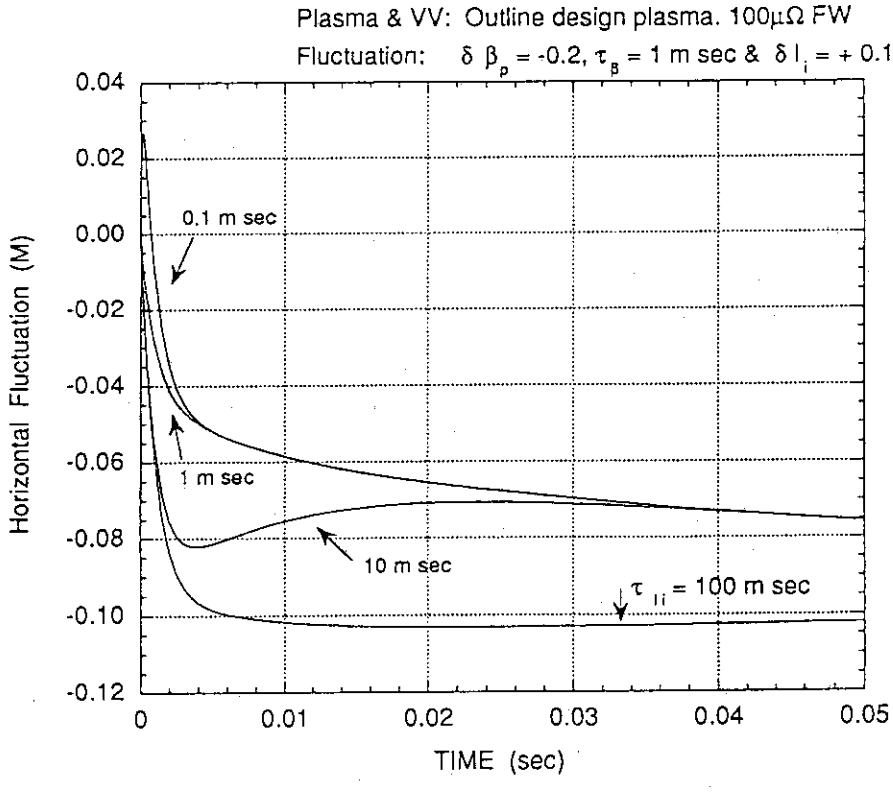

Fig. 19-2 The time constant of $\delta \ell_i$ vs. the horizontal motion for $\delta \ell_i$ increase.

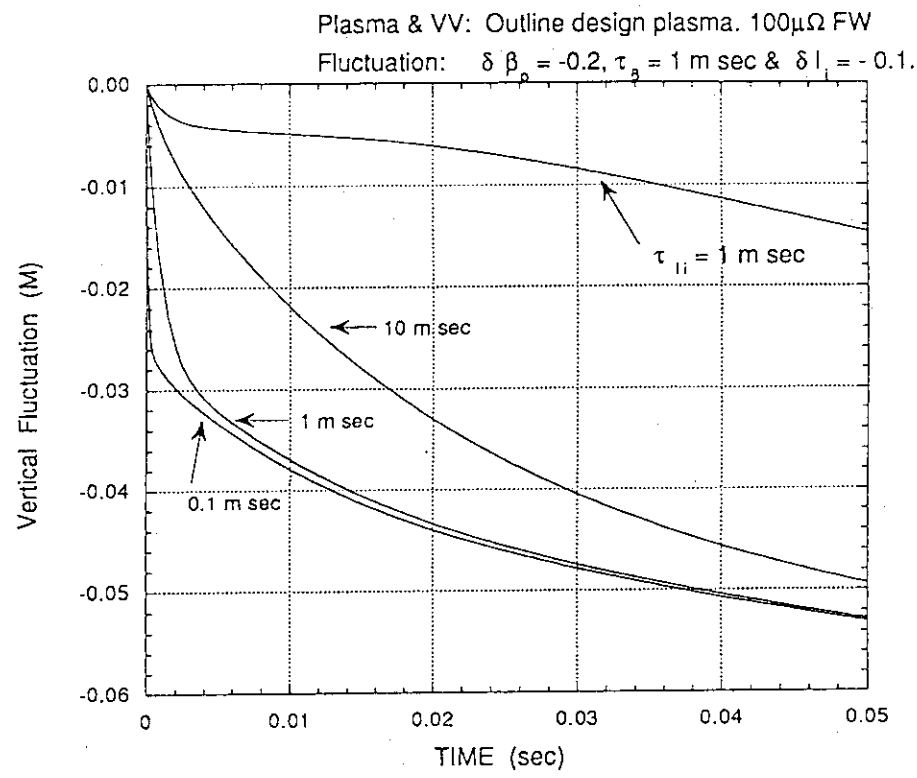

Fig. 20-1 The time constant of $\delta \ell_i$ vs. the vertical motion for $\delta \ell_i$ drop.

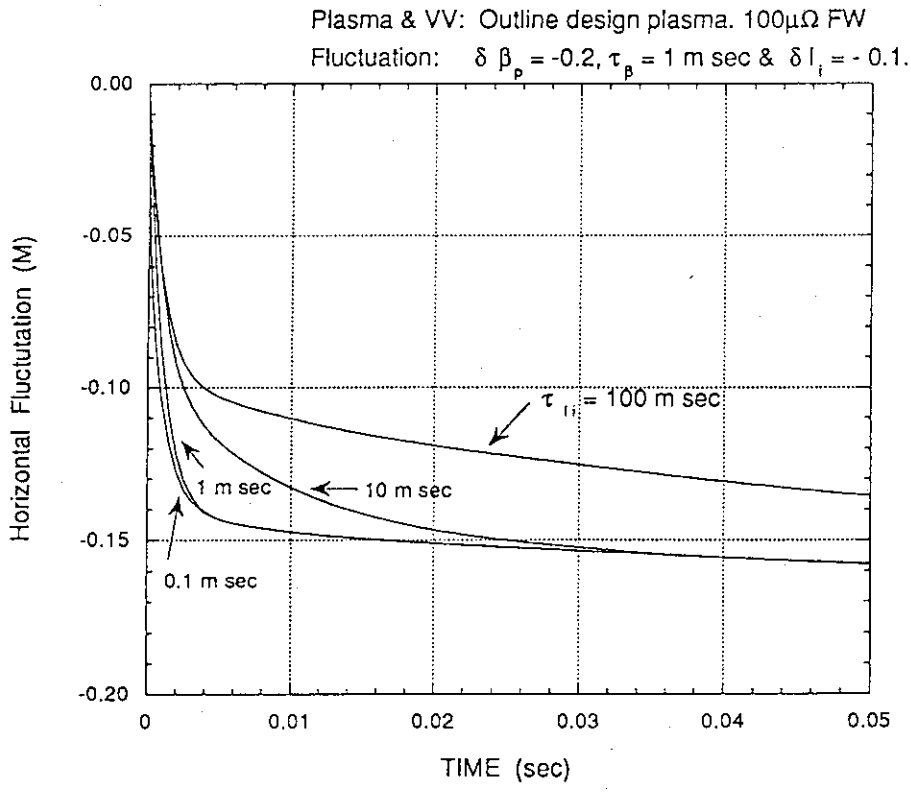

Fig. 20-2 The time constant of $\delta \ell_i$ vs. the horizontal motion for $\delta \ell_i$ drop.

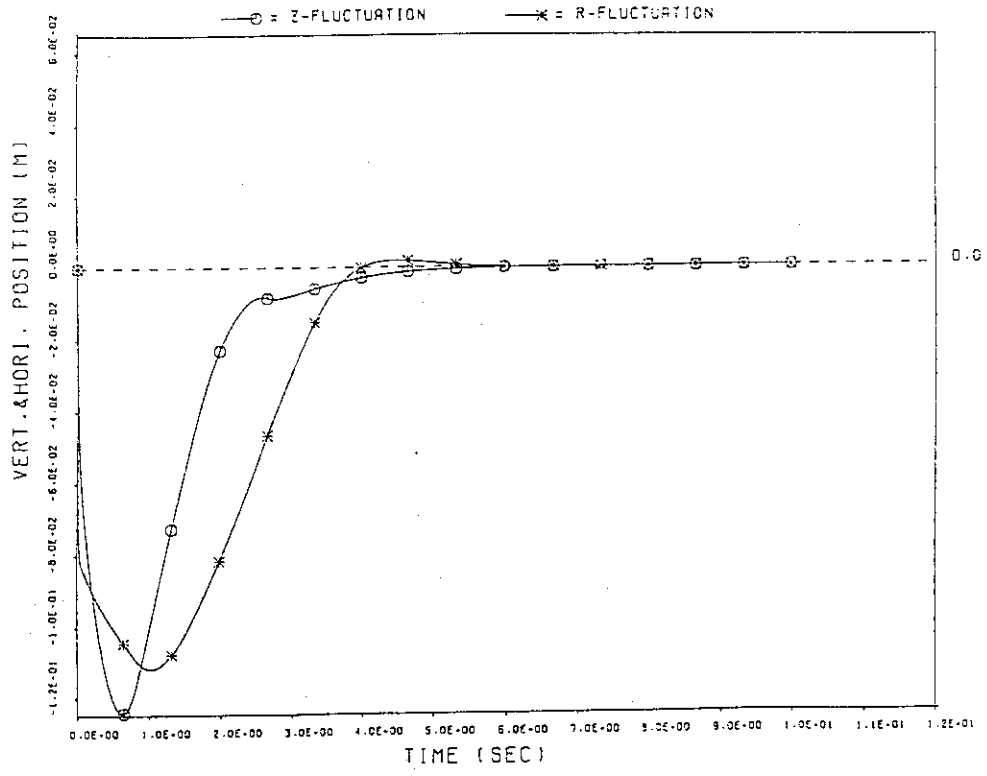

Fig. 21-1 Vertical and Horizontal plasma fluctuations

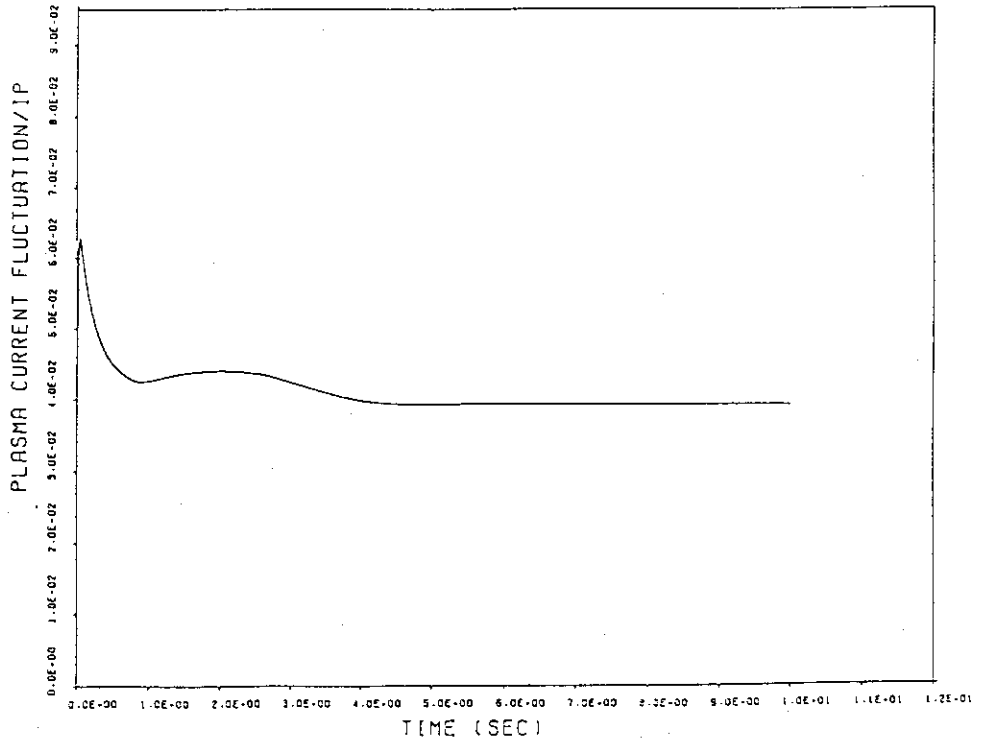

Fig. 21-2 Plasma current fluctuations

Fig. 21 Similation of the position control when 10 % drops of $\delta\beta_p$, $\delta\ell_i$ occur (Plasma = Outline Design, $\tau_{\beta_p} = 10$ msec, $\tau_{\ell_i} = 10$ msec, $Z_0 = 1$ cm, limit voltage = 10 V)

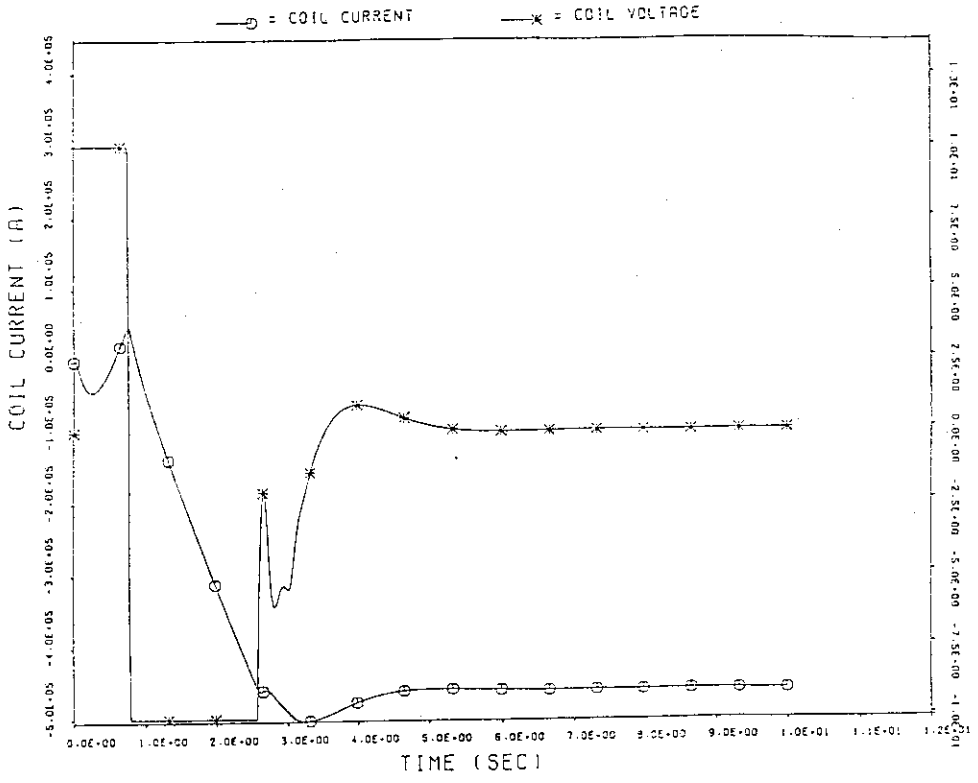

Fig. 21-3 The current and voltage of PF1

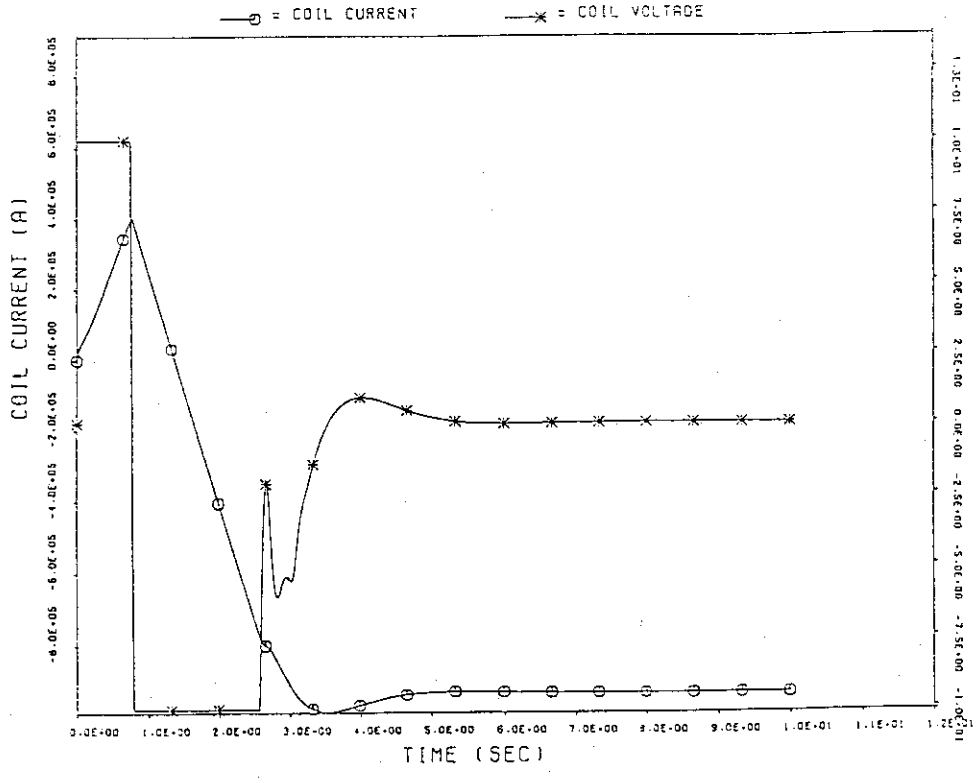

Fig. 21-4 The current and voltage of PF2

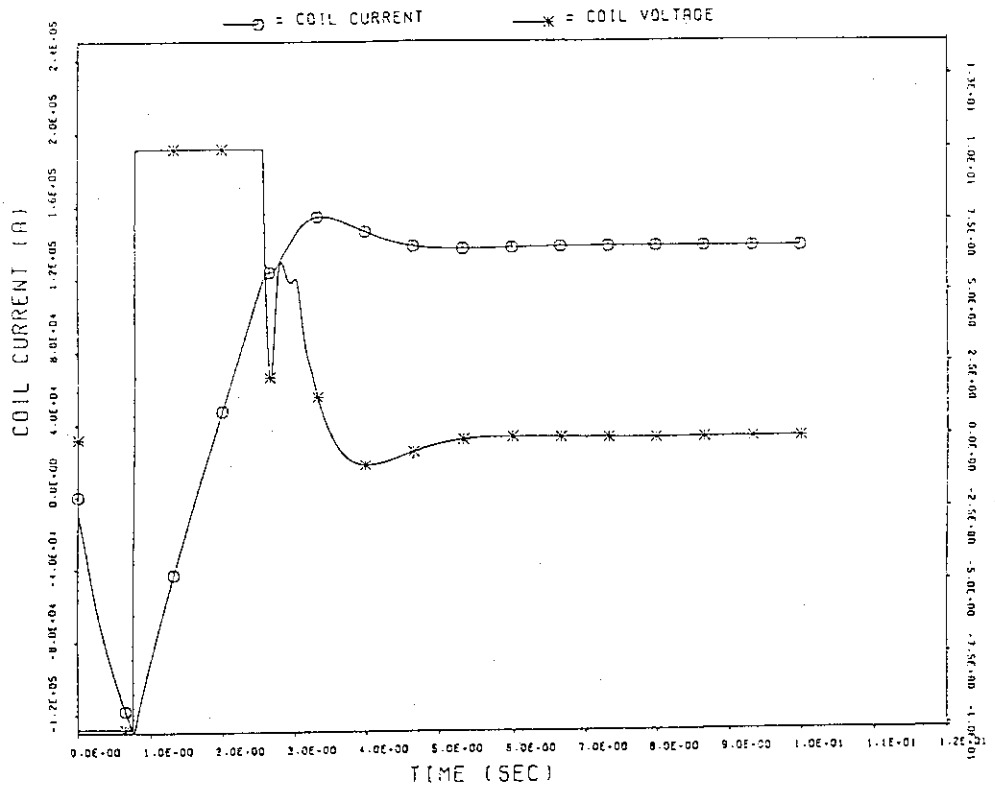

Fig. 21-7 The current and voltage of PF5

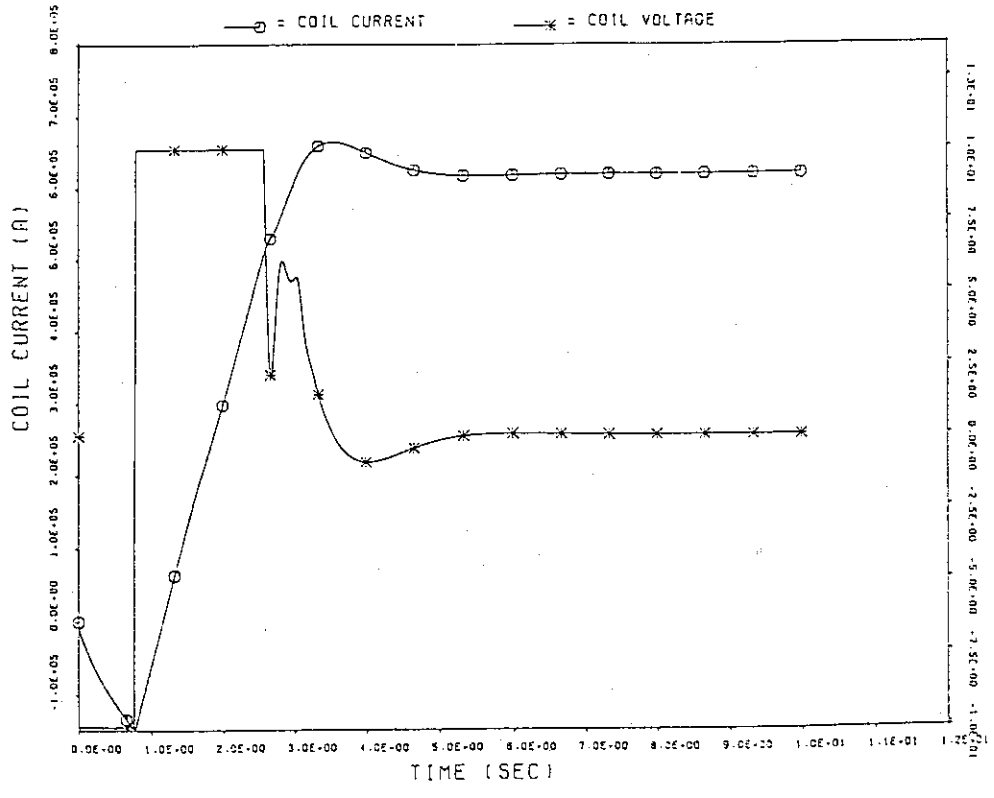

Fig. 21-8 The current and voltage of PF6

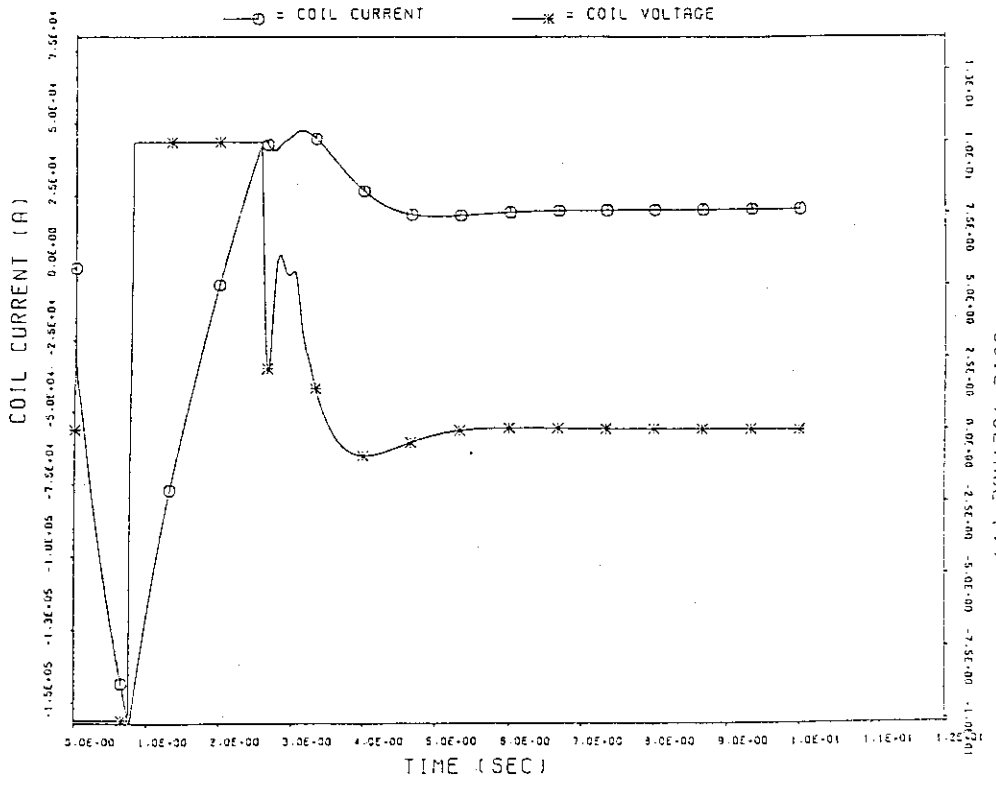

Fig. 21-5 The current and voltage of PF3

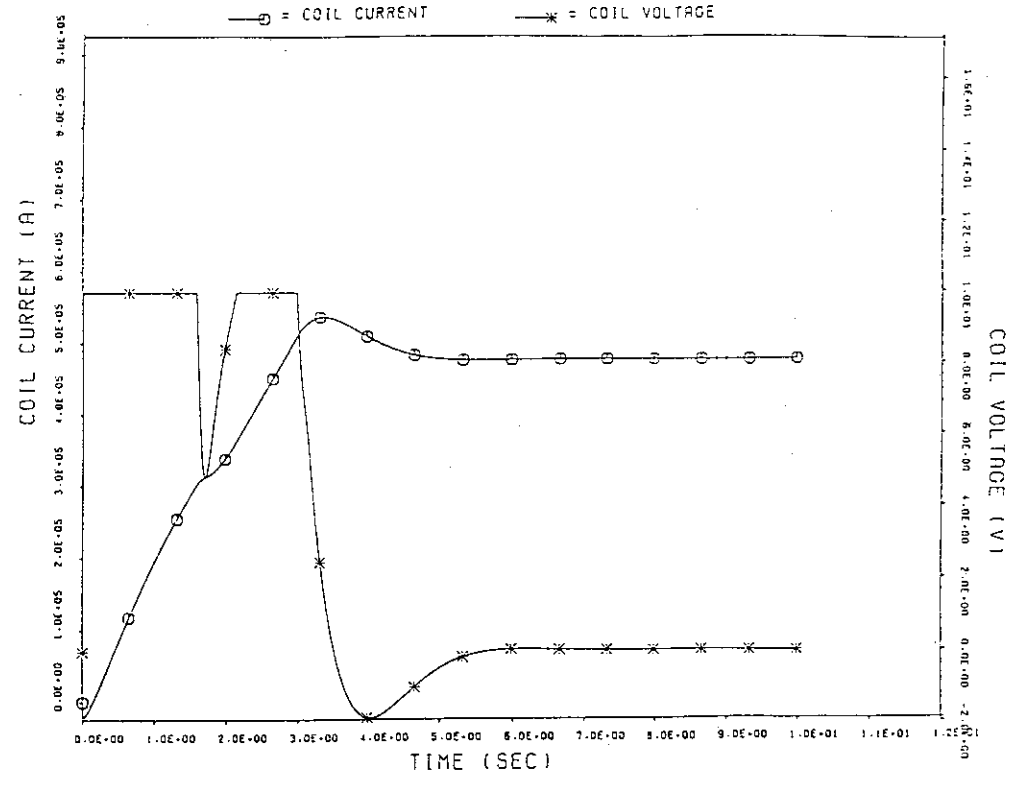

Fig. 21-6 The current and voltage of PF4

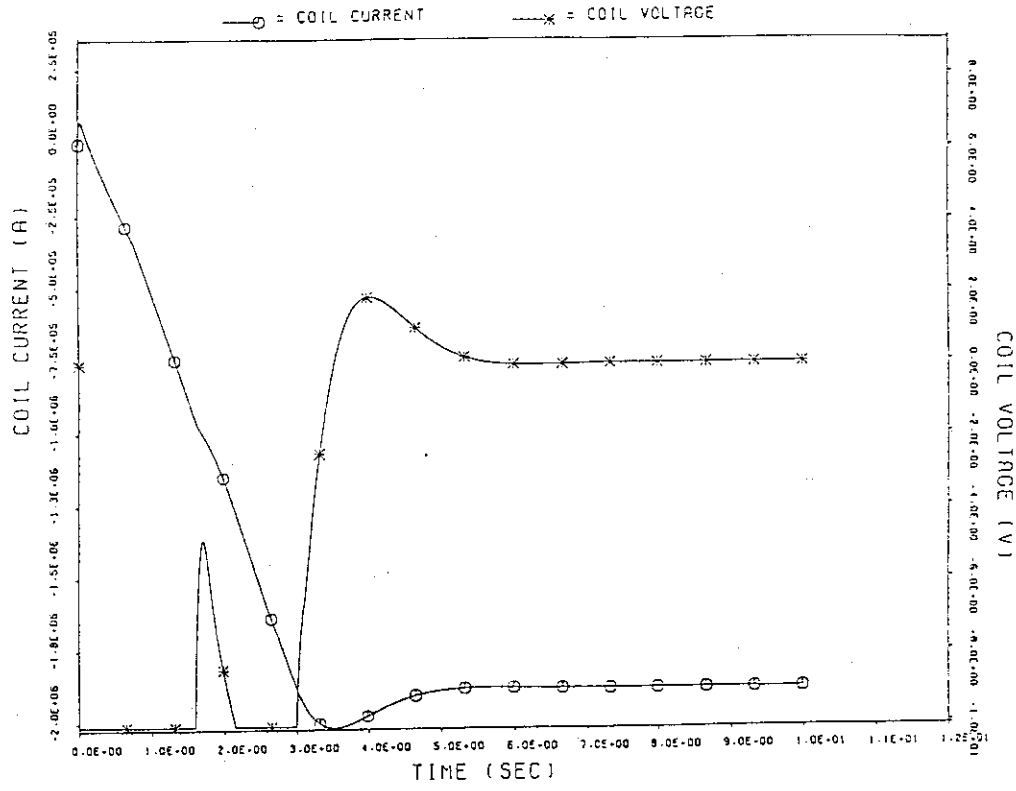

Fig. 21-9 The current and voltage of PF7

Appendix

In this section, Eqs.(18) and (19) are derived. The contributions of the change in the plasma current profile to the linearized equation is derived from Eq.(6). When the plasma current density changes as

$$i_p \rightarrow i_p + \delta i_p \quad ,$$

the equation of the vertical motion of plasma in Eq.(6) becomes

$$M_p \ddot{Z}_p = -\int dRdZ\, 2\pi R \left(i_{p(R,Z)} + \delta i_{p(R,Z)}\right) B_{R(R,Z)} \quad .$$

Because the vertical force on the plasma is balanced in the equilibrium, Eq.(12), only the contribution from δi_p remains. Since we assume that δi_p and $(\delta Z, \delta R)$ are first order quantities, combinations between them do not appear in the linear approximation.

The horizontal equation is derived similarly. The dependence on the internal inductance appears explicitly in the Shafranov term. The contribution from vertical field appears from the term

$$\int dRdZ\, 2\pi R \left(i_{p(R,Z)} + \delta i_{p(R,Z)}\right) B_{Z(R,Z)} \quad .$$

Since the unperturbed term balances with the Shafranov term in the equilibrium, only the first order term with respect to δi_p contributes. In order to express the change of plasma current profile by the internal inductance, we define $(\partial_{\ell_i} F_Z, \partial_{\ell_i} F_R)$ by Eq.(19), where $\delta \ell_i$ is the change of the internal inductance when the plasma current profiles is modified by δi_p.

The modifications to the circuit equation Eq.(13) appear in the plasma self-inductance and plasma-(coil,eddy mode) couplings. These contributions appear in the third element and below in Eq.(18). In our formulation, we use the change of the internal inductance in stead of using plasma current density δi_p. In this sense, we disregard the effects to the equation of motion which are not expressed in terms of the internal inductance.